ITINERIS

Geophysical methods in geoscience and near surface geophysics
Electrical Prospecting

Pisa, 21 January 2025

- Azadeh Hojat (azadeh.hojat@polimi.it)

IR0000032 – ITINERIS, Italian Integrated Environmental Research Infrastructures System
(D.D. n. 130/2022 - CUP B53C22002150006) Funded by EU - Next Generation EU PNRR-Mission 4 “Education and Research” - Component 2: “From research to business” - Investment 3.1: “Fund for the realisation of an integrated system of research and innovation infrastructures”

Finanziato dall'Unione europea NextGenerationEU

Ministero dell'Università e della Ricerca

Italiadomani

Syllabus

Electrical Prospecting (6 hours):

- Mechanisms of electrical conduction in rocks
- Ohm's law
- Archie's law
- Field generated by a point electrode on the surface of a homogeneous and isotropic half-space
- Electric quadripole and apparent resistivity
- Electrode arrays
- Vertical electrical soundings
- Horizontal electrical transversing
- Electrical resistivity tomography
- Hints on interpretation
- Examples

Electrical and electromagnetic methods

ITINERIS

Electrical properties of the earth can be explored either by electrical methods where direct currents or low frequency alternating currents are applied or by electromagnetic methods which apply electromagnetic induction phenomenon and the wave character of the electromagnetic field.

Direct current methods
- **Natural fields**
  - Self-potential method
- **Artificial fields**
  - DC resistivity
  - Induced polarization

Alternating field methods
- **Natural fields**
  - Magnetotelluric method
- **Artificial fields**
  - Conductivity meter
  - Tilt-angle method
  - VLF
  - TDEM

The variety of available techniques is much greater than in other geophysical methods.

- **Resistivity** is the physical property that is mainly involved in this kind of surveys.
- In some cases, importance may be given to other properties: **magnetic permeability** (low frequency), **permittivity** (high frequency)

Historical notes

1720: Gray and Wheeler made electrical studies of rocks and listed their electric conductivities

1830: First observation of natural electrical currents in copper mines by R. Fox

1882: C. Barus introduces the use of non polarizable electrodes for measuring natural potentials to detect ore bodies

1913-1920: Industrial use of the Self-potential method begins with C. Schlumberger

1912-1920: The method of resistivity measurements with 4 electrodes is introduced almost simultaneously by Wenner (1912-1917) and Schlumberger (1920)

1920: infancy of Induced Polarization (IP) method with the first observations of different potential decay curves in presence of particular bodies by Schlumberger

1922: introduction of the concept of apparent resistivity

Historical notes

Late 1930s: development of theoretical curves of self-potentials for simple models (e.g., 2 or 3 horizontal layers)

Late 1940s: industrial use of the IP method begins

1950: development of IP measurements in the frequency domain

1960s and 1970s: development of numerical methods for potential modelling and development of automatic inversion methods

1990s: development of multielectrode systems for fast acquisitions; development of capacitive-coupled electrodes

Recent couple of decades: development of autonomous ERT monitoring systems

Self potential (SP) method

- **Passive method**
- **Measurements of naturally occurring electrical potentials**
- **Common applications:**

Mapping sulfide ore bodies, detection of leakage zones in the buried walls of earth dams, exploration of karstic springs, water table investigations, geothermal

SP and resistivity graphs over a fissured zone of limestone, following the infiltration of precipitation or irrigation water.

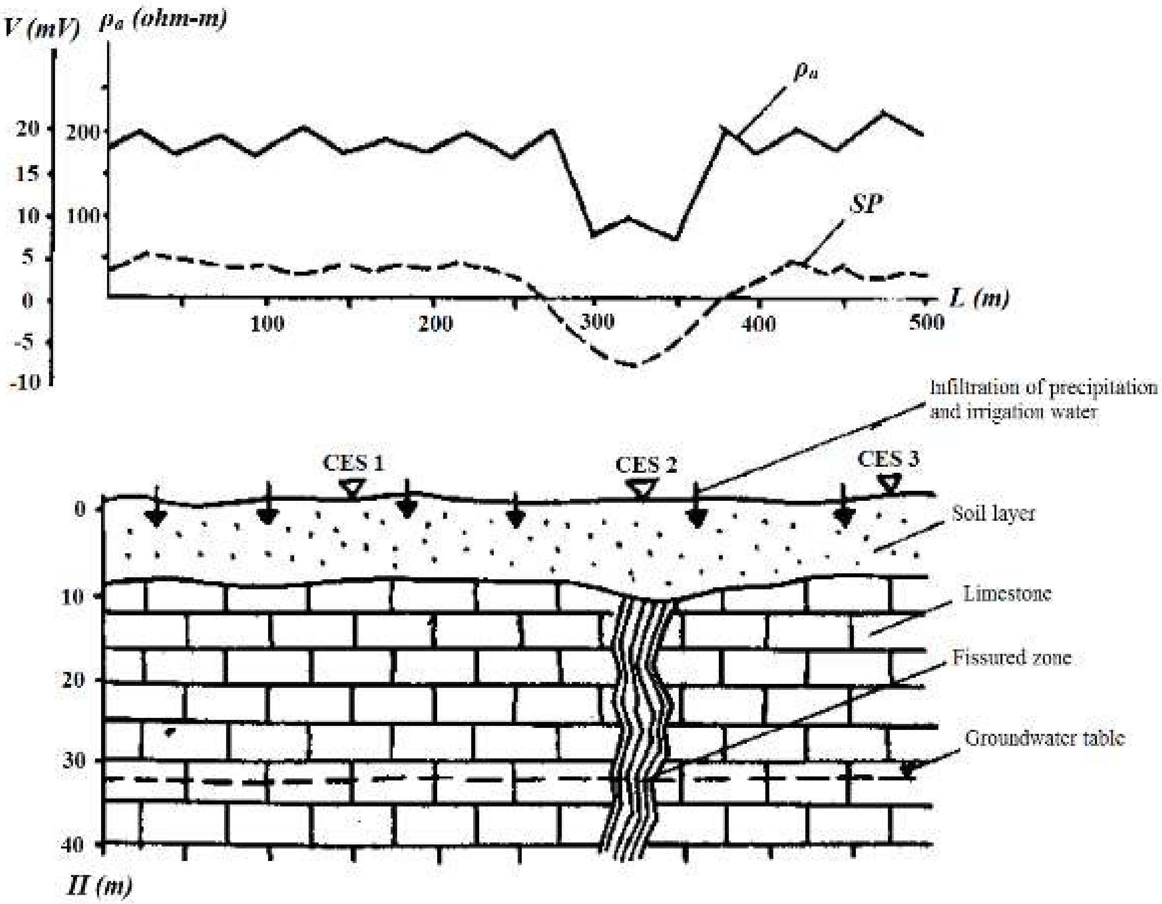

(Ogilvy and Bogoslovsky, 1979)

DC resistivity method

- **Active method**

- **Electrical current flow generated by a DC, or slowly varying AC, source**
- **Measurements of electrical potential**

- **<u>Common applications</u>:**
Mapping presence and quality of pore fluids and clays, detection of the depth to bedrock, near surface geophysical mapping, exploration of metallic minerals

a) Resistivity sounding positions along a proposed route of road construction. (b) Interpretation of resistivity soundings along the road site investigation rout .

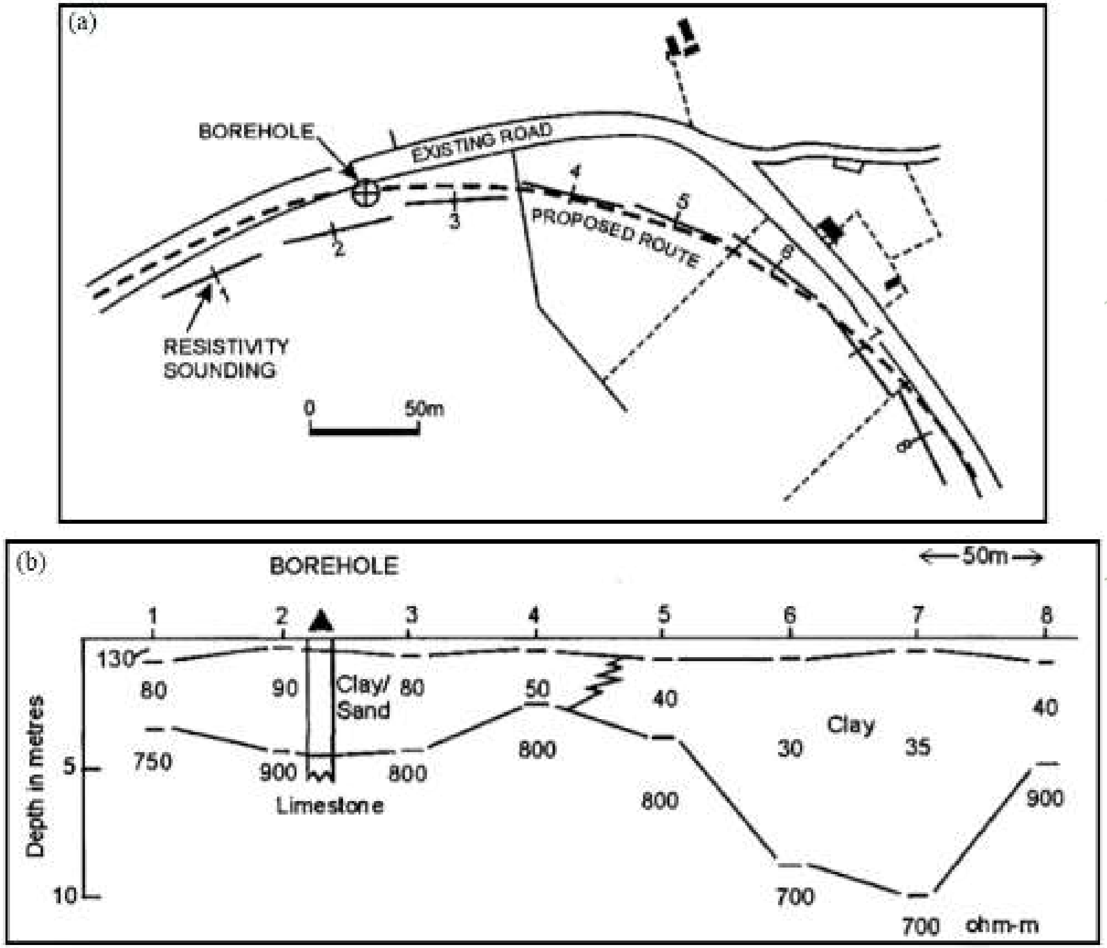

(McDowell et al., 2002)

Induced polarization (IP) method

- **Active method (usually done in conjunction with DC resistivity)**

- **Current is initially applied or removed from the ground**
- **Measurements of the transient variations in potential (the ground behaves like a capacitor)**

- **<u>Common applications</u>:**
Search for disseminated metallic ores and, to a lesser extent, groundwater (detecting concentrations of clay), and geothermal exploration

Resistivity and IP curves showing clay horizons.

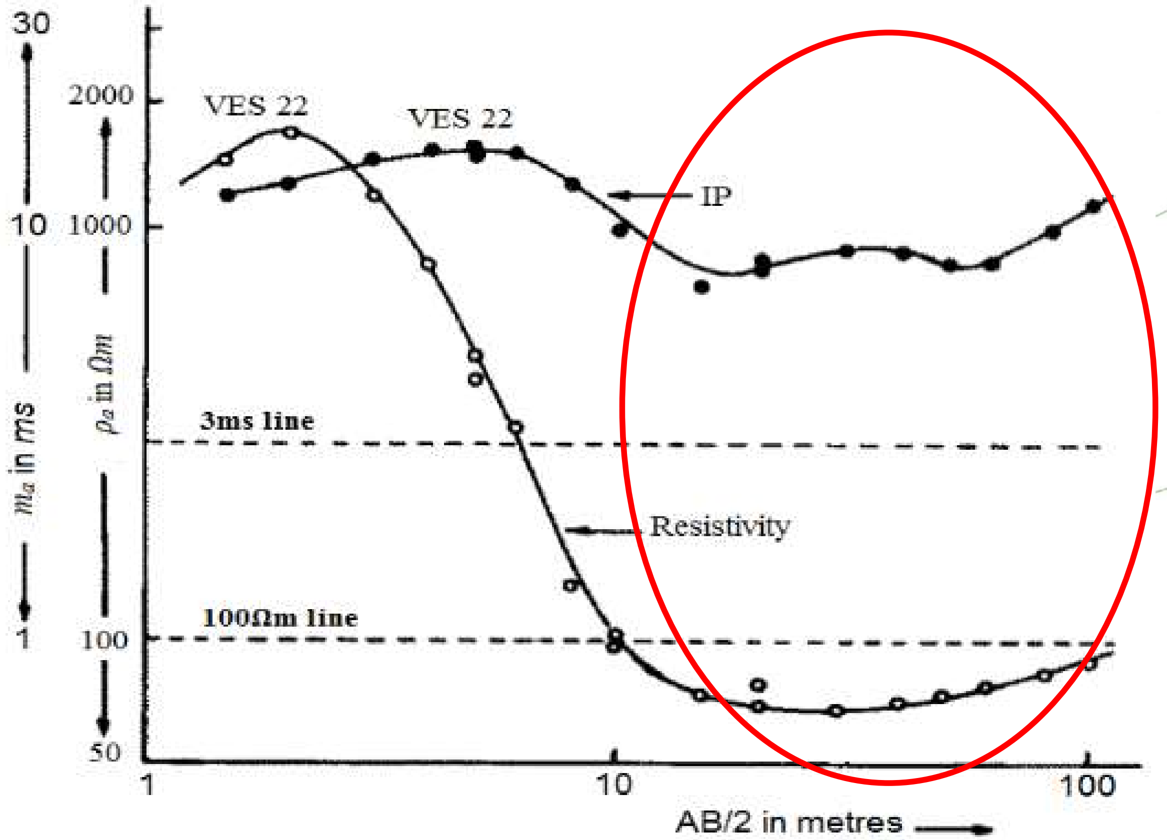

(Roy and Elliott, 1980)

Electrical properties: Resistance and Resistivity

Resistivity is the property of a material that resists the flow of electrical current.

Ohm's Law: the current through a conductor between two points is directly proportional to the potential difference across the two points

$$R = \frac{\Delta V}{I} = \rho \frac{l}{A}$$

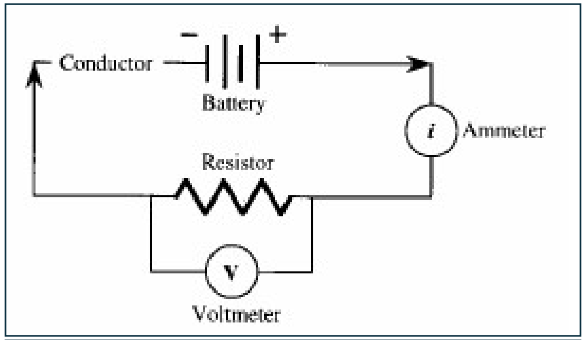

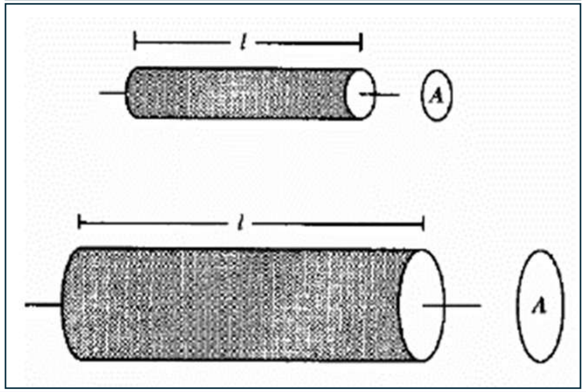

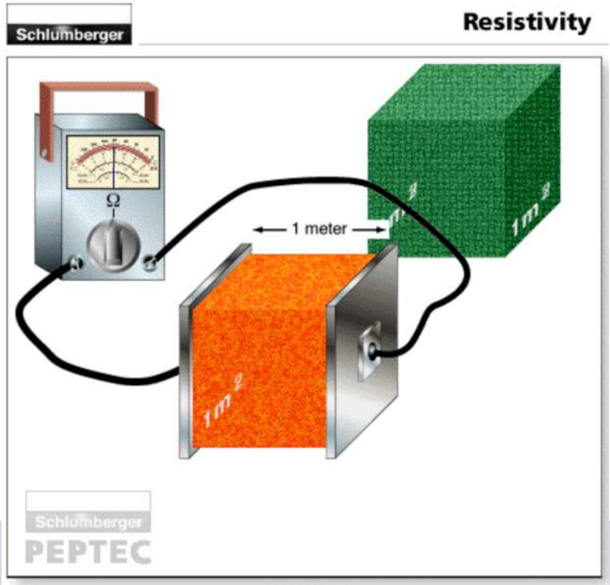

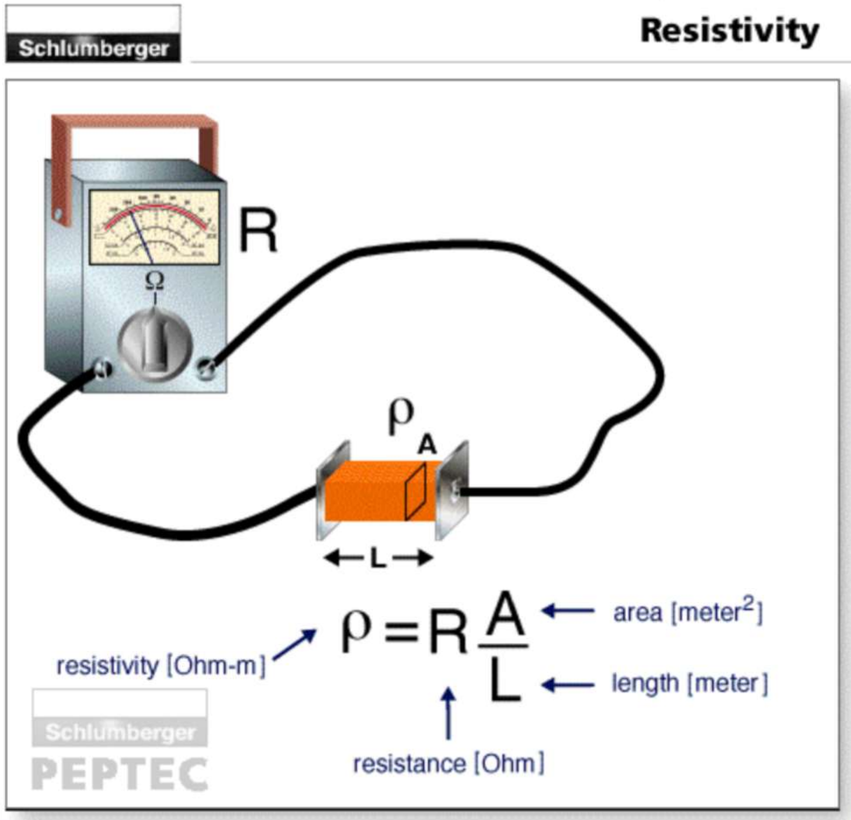

Electrical properties: Resistivity

Ohm's law in differential form:

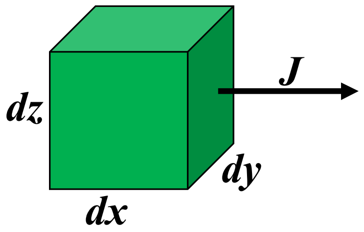

$$R = \frac{\Delta V}{I} = \frac{E \cdot dx}{J \cdot dy \cdot dz} = \rho \frac{dx}{dy \cdot dz}$$

Hence: $$\boxed{E = \rho \cdot J}$$

$E \Rightarrow$ electrical field

$J \Rightarrow$ current density

N.B.: ρ is scalar only in case of isotropic materials.

In rocks, resistivity depends on:

- ❑ **Minerals**
- ❑ **Fluid content in pores and fractures**

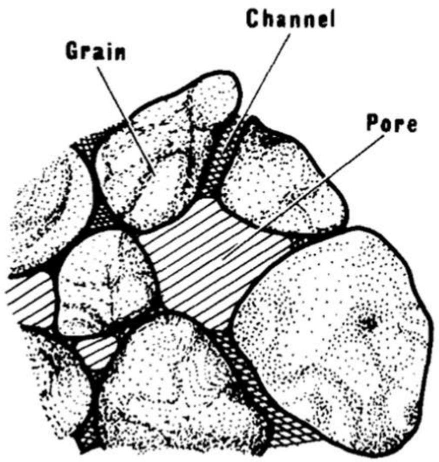

Most soils and rocks are essentially nonconductive, thus in most earth materials the conduction of electric current takes place virtually entirely in the water occupying the pore spaces or fractures.

Resistivity of minerals

Minerals can be subdivided into 3 subsets:

Metallic conductors: Conduction is due to the presence of atoms having loosely held valence electrons. Impurities and thermal agitation of ions obstruct conduction.

Typical range of values: $10^{-6} < \rho < 10^{-3}\ \Omega m$

Examples: gold, copper, tin, platinum, silver, graphite

ρ increases with increasing temperature and impurities

Semiconductors: Charge is carried by electrons. They are normally fixed in the atomic lattice, but can be displaced by using thermal energy.

Examples: sulphides (e.g., pyrite, chalcopyrite, bornite, $10^{-5} < \rho < 10^{-2}\ \Omega m$), metal oxides ($10^{-2} < \rho < 10\ \Omega m$)

ρ decreases with increasing temperature

Dielectrics: They are the most common minerals in the lithosphere (silicates, sulphates, carbonates….).
Current is carried by ions either removed from the lattice by means of thermal agitation or consisting of impurities.

$10^{6} < \rho < 10^{14}\ \Omega m$

ρ decreases with increasing temperature

Resistivity of fluids

Fluids contained in rocks:

- **Air**
- **Water (with different salt concentrations)**
- **Hydrocarbons (in liquid or gaseous state)**

Air and hydrocarbons have very high resistivity.

Water resistivity depends on:

- ***Dissolved salts***
- ***Salt concentration***
- ***Temperature***

Sodium chloride is the most common salt that can be found in underground water. Multipliers are available for the conversion of some ionic concentrations to their NaCl equivalents.

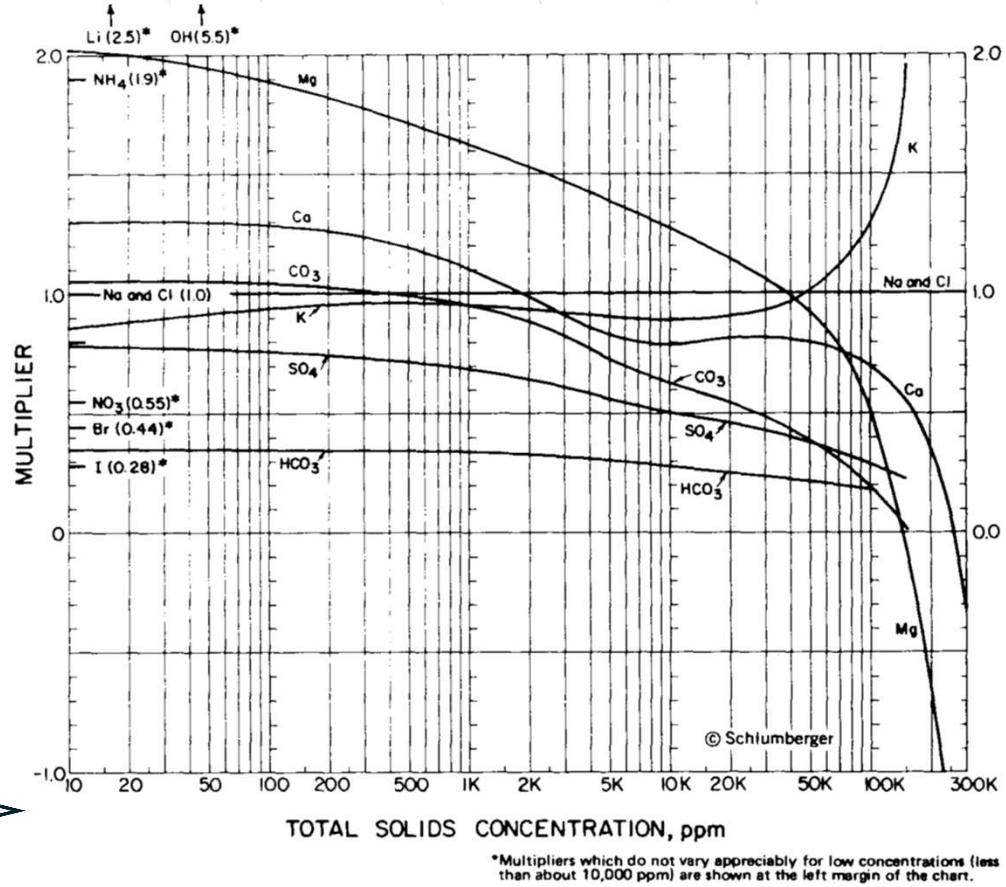

Resistivity of solutions

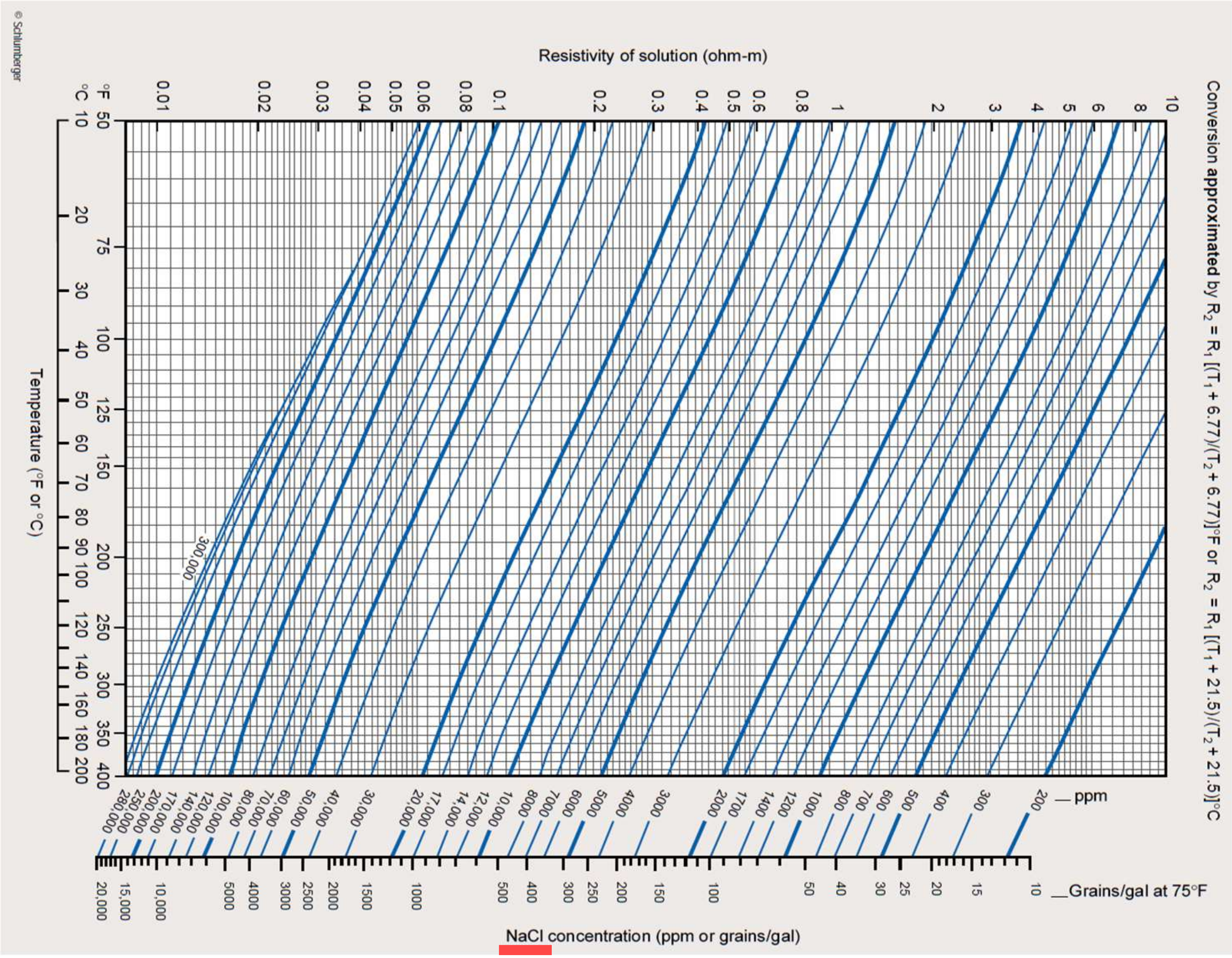

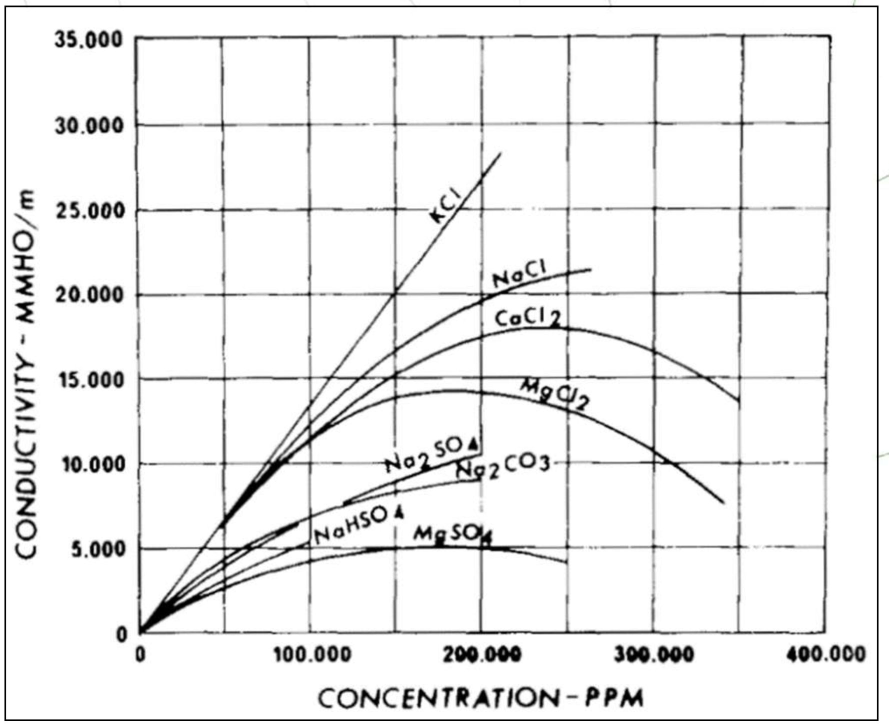

(Serra, 1984)

Resistivity of porous/fractured rocks with water

Water-saturated permeable rocks with dielectric grains (e.g., sands, sandstones, limestones….)

Shape as well as dimension of pores and fractures allow to create a continuous network through which water is free to flow.

In this case the bulk rock resistivity is:

$$\rho = F\rho_W$$

ρ_w= pore water resistivity

F = Formation factor of the rock

F increases with decreasing porosity, according to an empirical relationship (Archie's law):

$$F = a\phi^{-m}$$

φ = porosity (pore volume/total volume)

a, m = empirical constants ($0.5 < a < 2.5$; $1.3 < m < 2.8$)

If rock is not 100% water-saturated, Archie's law thus becomes:

$$\rho = F\rho_W S_w^{-n}$$

S_w = water saturation (water volume/pore volume)

n = saturation factor (empirical constant ranging between 1.5 and 2.2)

Common average resistivity values

Soils	resistivity in Ωm
Dry sands and gravels without clay content	> 1000
Saturated sands and gravels, conglomerates, without clay content	100 -500
Saturated sandy limes	30 -100
Clay limes	20 - 50
Alluvial or lacustrine clays	5 - 20
Marine clays	1 - 10
Igneous rocks	
Dry young lava (Etna)	> 20000
Unaltered lapideous igneous rocks	> 1000
Unaltered saturated pyroclastic tuffs	> 500
Highly argillaceous igneous rocks	> 5
Sedimentary and metamorphic rocks	
Saturated, fractured and clean limestones and dolomites	> 1000
Argillaceous limestones	100 - 300
Calcareous marls	50 - 100
Marls	20 - 40
Schists and non phyllitic or argillaceous metamorphic rocks	> 500
Argillaceous schists or altered phyllitic schists	20 - 50

Note the overlap between resistivity values of different material.

Electrical properties

Permittivity

$$C = \varepsilon \frac{A}{l}$$

C = capacitor's capacitance
A = surface area of the plate
l = distance between the plates
ε = permittivity

$$\varepsilon_{vacuum} = 8.85 \times 10^{-12} \frac{F}{m}$$

- **Usually given in relative values referred to ε_{vacuum}**
- **For most rocks: $4 < \varepsilon_r < 10$**
- **Its value can increase considerably: $\varepsilon_{r,water}=80$**

Magnetic permeability

When EM sources are employed, the voltage induced in a subsurface conductor varies not only with the rate of change of magnetic field, but also with the magnetic permeability of the conductor.

$$\nabla \times E = -\mu \frac{\partial H}{\partial t}$$

$$\mu_{vacuum} = 4\pi \times 10^{-7} \frac{H}{m}$$

The magnetic permeability of nearly all rock formations, with the exception of few particular cases (rocks with magnetic properties), is the same of vacuum.

Electric potential

Consider a single current point source which supplies a current of intensity *I* in a homogeneous medium of resistivity *ρ*.

$$\nabla^2 V = 0$$

Laplace's equation

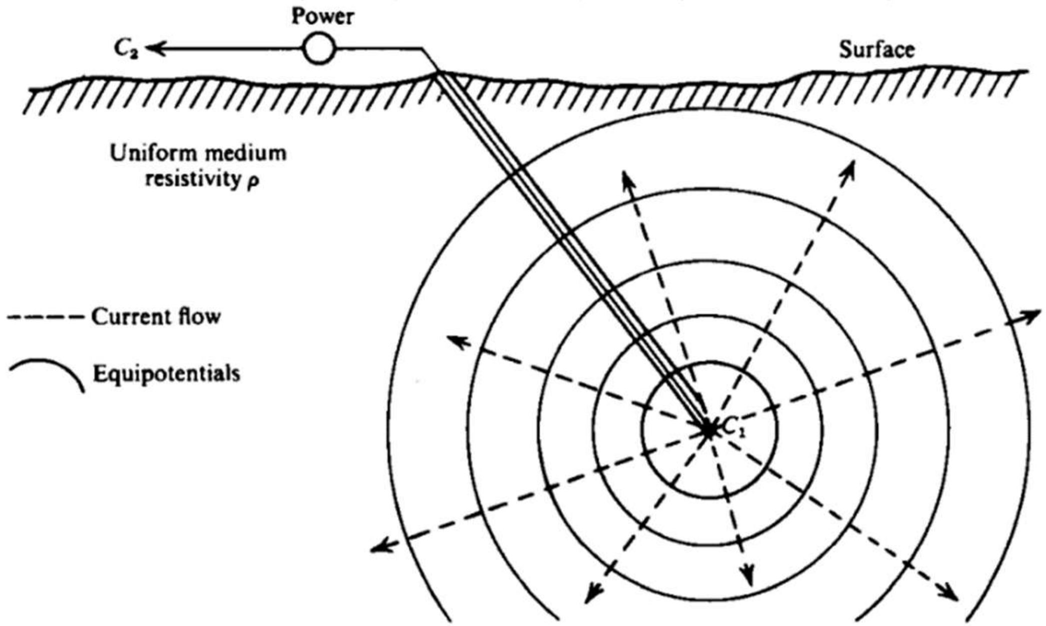

Laplace's equation in spherical coordinates:

$$\nabla^2 V = \frac{1}{r^2}\frac{\delta}{\delta r}\left(r^2\frac{\delta V}{\delta r}\right) + \frac{1}{r^2 \sin\theta}\frac{\delta}{\delta\theta}\left(\sin\theta\frac{\delta V}{\delta\theta}\right) + \frac{1}{r^2\sin^2\theta}\frac{\delta^2 V}{\delta\varphi^2} = 0$$

Electric potential

Since there is spherical symmetry:

$$\frac{\delta V}{\delta \varphi} = 0 \qquad \frac{\delta V}{\delta \theta} = 0 \qquad \Rightarrow \qquad \nabla^2 V = \frac{\delta^2 V}{\delta r^2} + \frac{2}{r}\frac{\delta V}{\delta r} = 0$$

The solution to the equation is of the form: $V = \frac{A}{r} + C$ **where *A* and *C* are constants**

Assuming *V = 0* when $r \to \infty$**, we obtain *C = 0*** **Because of symmetry, at distance *r* we have:** $J = \frac{I}{4\pi r^2}$

and then $E = \rho \cdot J = \rho \frac{I}{4\pi r^2}$ **Considering that:** $E = -\frac{\delta V}{\delta r} = -\frac{\delta}{\delta r}\left(\frac{A}{r}\right) = \frac{A}{r^2}$

we obtain $A = \frac{\rho \cdot I}{4\pi}$

And therefore $V = \frac{\rho \cdot I}{4\pi}\frac{1}{r}$

The solution is unique according to the uniqueness theorem. In case of fields generated by more than one point source, we can apply the superposition principle.

Electric potential: Image source method

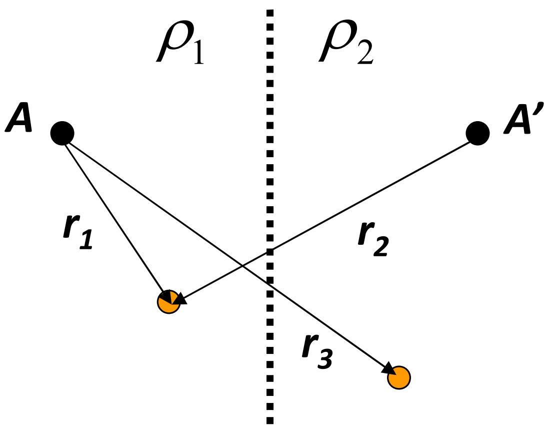

A → current source with intensity ***I***

A’ → **image source (delivering current with intensity *KI*)**

$$K = \frac{\rho_2 - \rho_1}{\rho_2 + \rho_1}$$ → **Reflection coefficient**

In medium 1: $$V_1 = \frac{\rho_1 I}{4\pi}\left(\frac{1}{r_1} + \frac{K}{r_2}\right)$$

In medium 2: $$V_2 = \frac{\rho_2 I}{4\pi}\frac{1-K}{r_3}$$

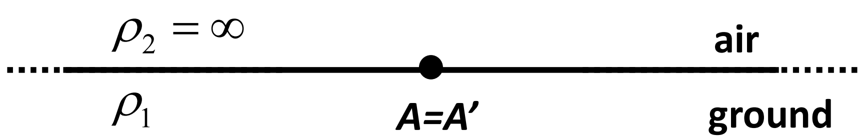

The image source overlaps with the real one

$$K = \frac{\rho_2 - \rho_1}{\rho_2 + \rho_1} = 1$$

So in medium 1, the ground, we have: $$V_1 = \frac{\rho_1 I}{4\pi}\left(\frac{1}{r} + \frac{1}{r}\right) \rightarrow V_1 = \frac{\rho_1 I}{2\pi}\frac{1}{r}$$

In case of 2 electrodes with opposite polarity: → $$V_1 = \frac{\rho_1 I}{2\pi}\left(\frac{1}{r_1} - \frac{1}{r_2}\right)$$

Self potential (SP) method

Certain natural or spontaneous potentials occurring in the subsurface are caused by electrochemical or mechanical activities.

Four principle mechanisms can produce natural potentials:

- *Electrokinetic potential*
- *Liquid junction (diffusion) potential*
- *Shale potential*
- *Mineralization potential*

SP method ranks as the cheapest of surface geophysical methods in terms of equipment necessary and amongst the simplest to operate in the field.

Two non-polarisable porous-pot electrodes are connected to a precision multimeter capable of measuring at least 1 *mV*.

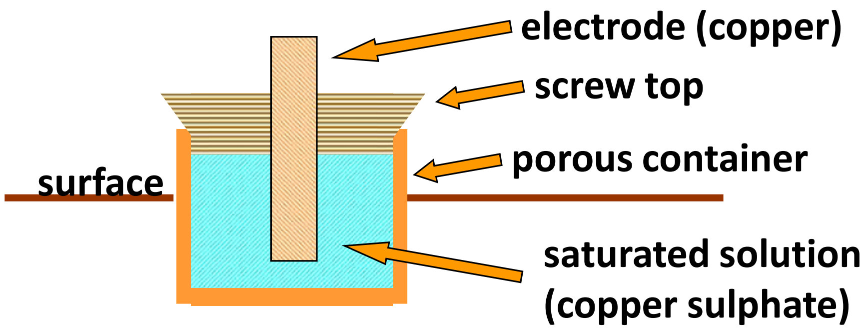

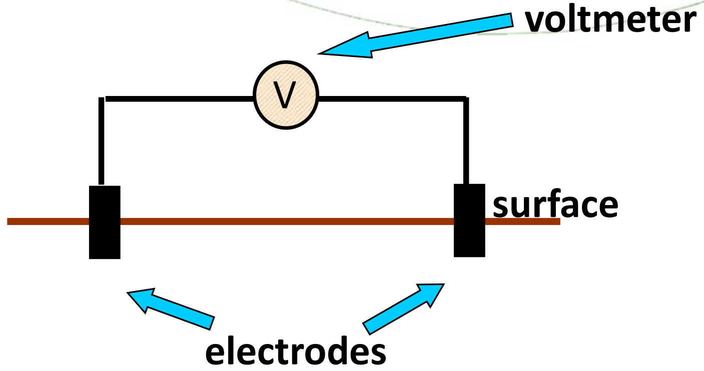

https://www.agiusa.com/non-polarizable-electrode

SP survey methods

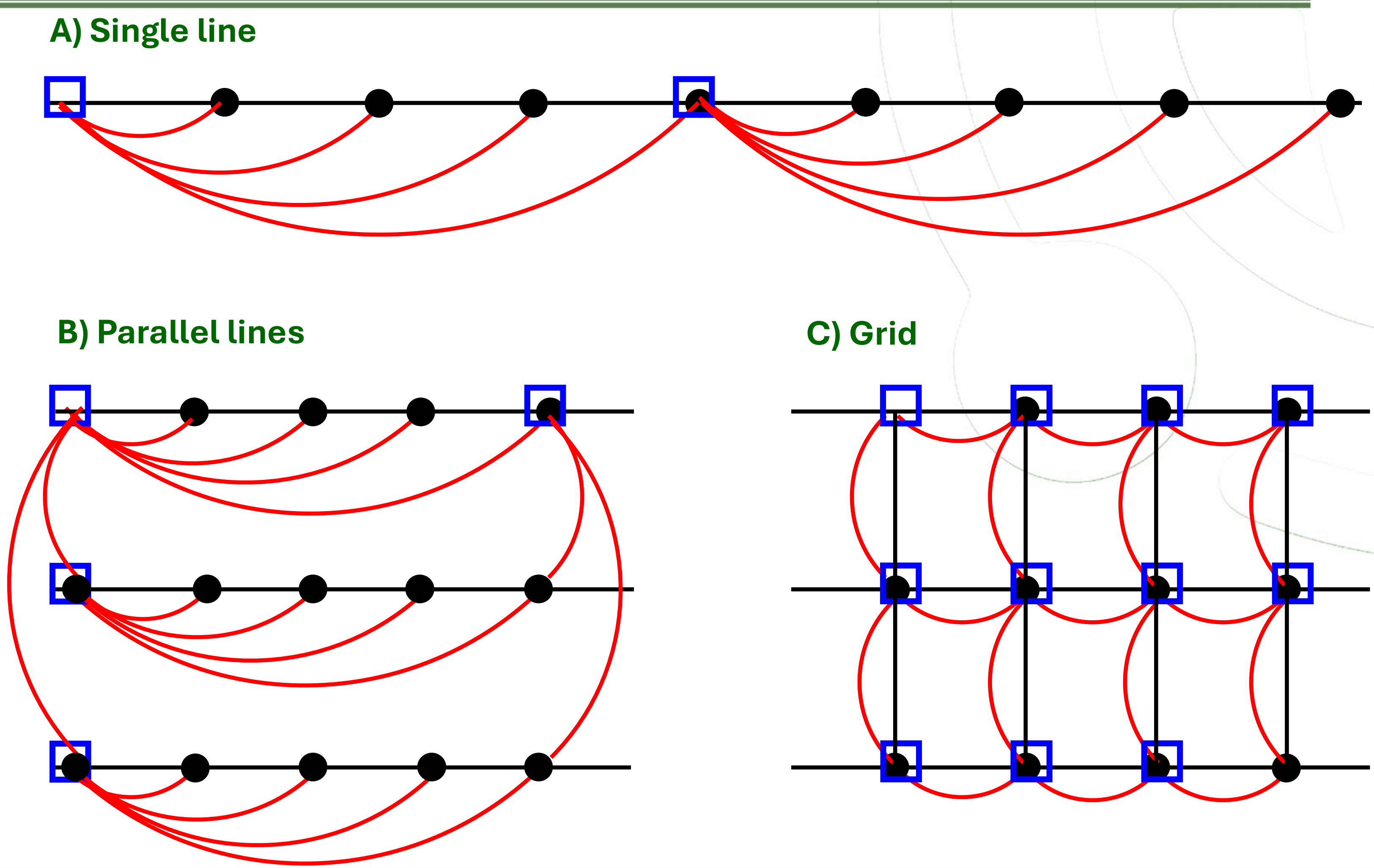

SP data display / interpretation

Aim: Metallic mineral exploration

Method: Detection of the minimum potentials (where ore bodies are supposed to be)
Comparison between observed potential curves and synthetic anomalies corresponding to a known model

Typical curves of SP generated by an ore body

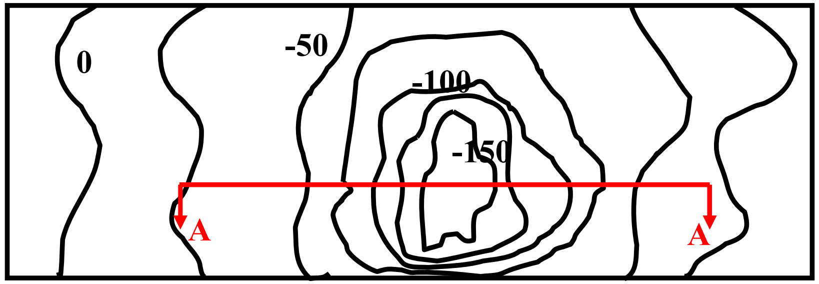

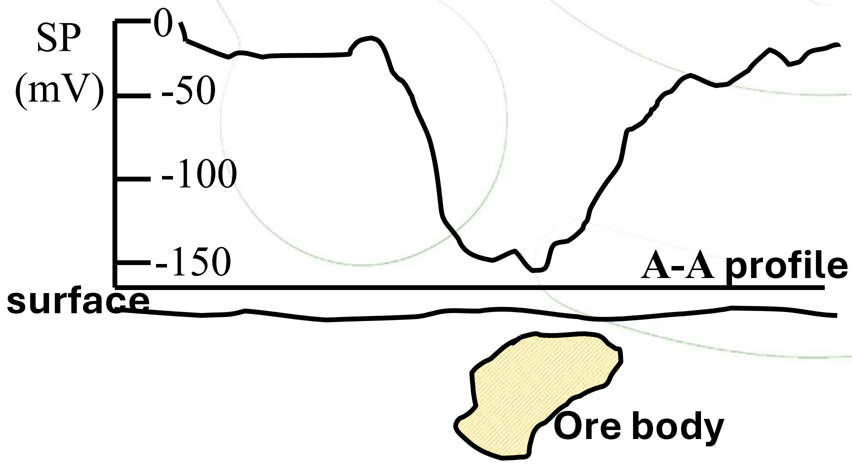

Qualitative interpretation:

- **SP anomalies are often interpreted qualitatively by profile shape, amplitude, polarity (+ or -) and contour pattern.**
- **The top of an ore body is assumed to lie directly beneath the position of the minimum potential.**
- **If the axis of polarization is inclined from vertical, the shape of the profile will become asymmetrical.**

SP example

Location of a massive copper ore body

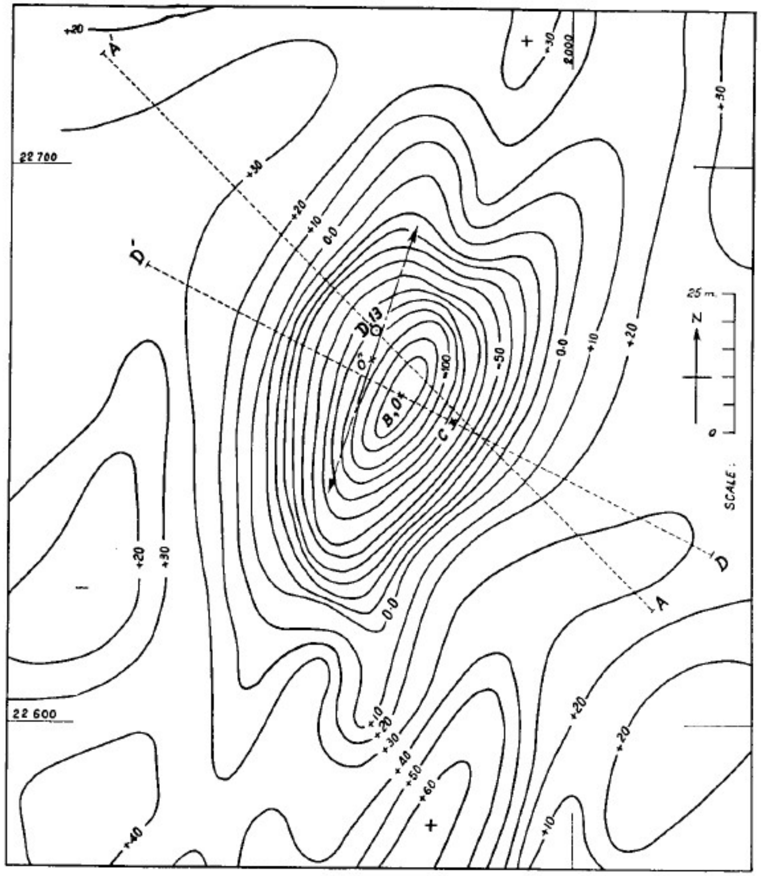

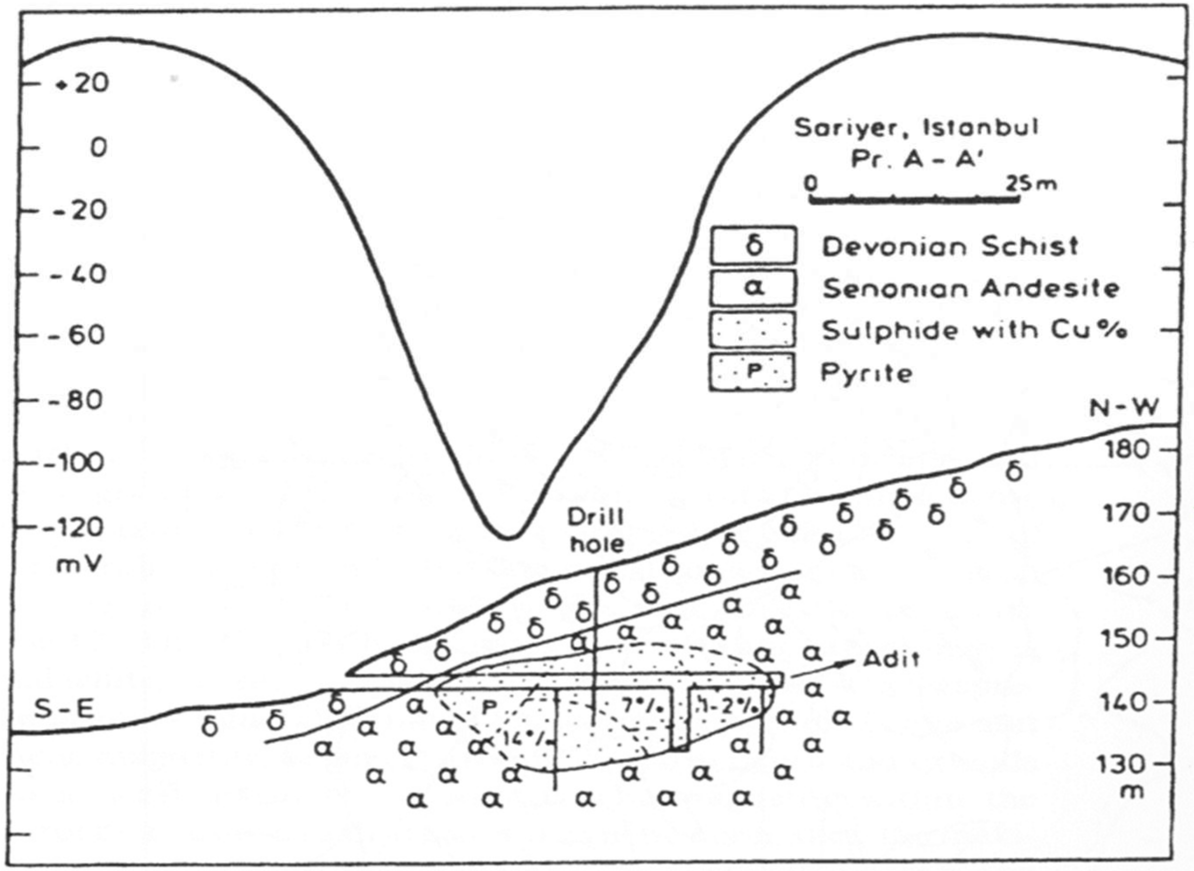

(Yungul, 1954)

DC resistivity method

A man-made electric field is generated in order to measure soil resistivity.

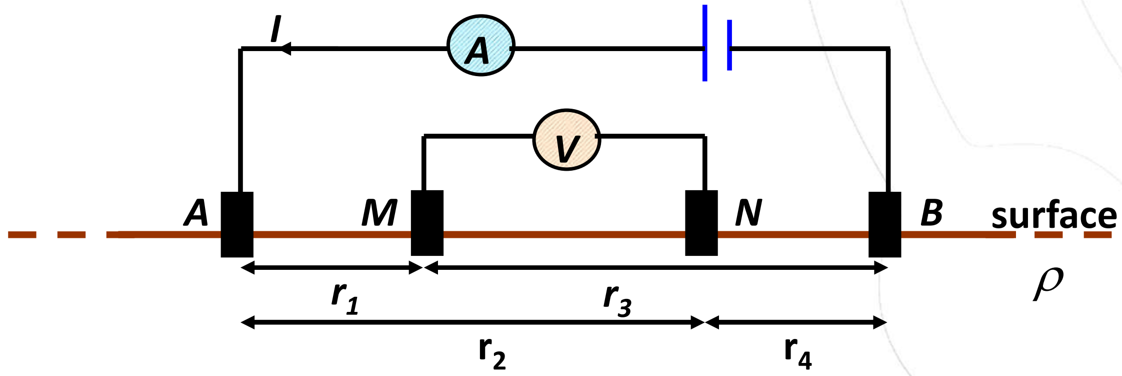

If sub-surface ground is homogeneous and isotropic:

$$V_M = \frac{\rho I}{2\pi}\left(\frac{1}{r_1} - \frac{1}{r_3}\right)$$

$$V_N = \frac{\rho I}{2\pi}\left(\frac{1}{r_2} - \frac{1}{r_4}\right)$$

$$\Delta V = V_M - V_N =$$

$$= \frac{\rho I}{2\pi}\left(\frac{1}{r_1} - \frac{1}{r_3} - \frac{1}{r_2} + \frac{1}{r_4}\right)$$

DC resistivity method

$$\rho = \frac{\Delta V}{I} 2\pi \frac{1}{\frac{1}{r_1} - \frac{1}{r_2} - \frac{1}{r_3} + \frac{1}{r_4}}$$

$$\rho_a = \frac{\Delta V}{I} C$$

I: **introduced current (*A*)**
ΔV: **measured potential difference (*V*)**
ρ_a: apparent resistivity (Ωm)
C: **geometrical factor**

N.B.: Once the subsurface is non-homogenous, the value determined for the resistivity is unlikely to equal the real resistivity of the material in which the electrodes are inserted. Therefore, the measured resistivity is termed "apparent resistivity".

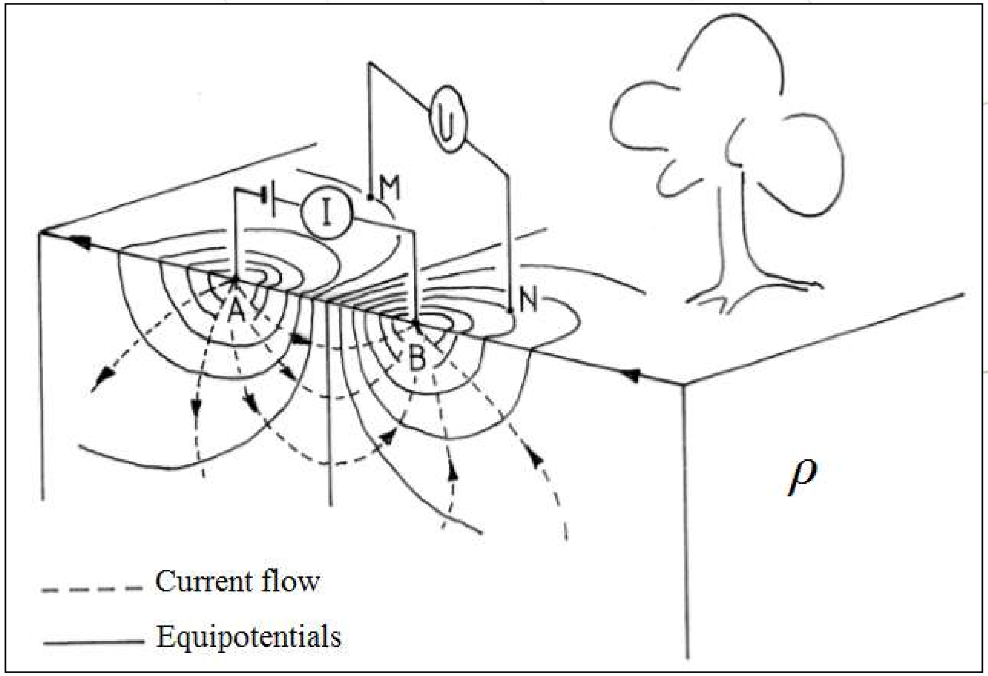

Electrode configuration (array)

The geometrical position of the four electrodes is called electrode configuration (array or arrangement).

Wenner Alpha: $C = 2\pi a$

Wenner Beta: $C = 6\pi a$

Wenner Gamma: $C = 3\pi a$

Schlumberger: when b>>a, $C = \pi b^2/a$

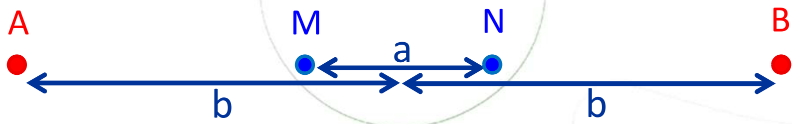

Wenner-Schlumberger: $C = \pi n(n+1)a$

Pole-Pole: $C = 2\pi a$

Pole-Dipole: $C = 2\pi n(n+1)a$

Dipole-Dipole: $C = \pi n(n+1)(n+2)a$

(modified from Loke, 2016)

Electrode configuration (array)

Wenner

- **High signal strength**
- **Good vertical resolution**
- **Moderate depth of investigation**

Dipole-dipole

- **Low signal strength**
- **Good lateral resolution**
- **Shallow depth of investigation**
- **No EM coupling effects**

Schlumberger

- **Moderate signal strength**
- **Moderate vertical and lateral resolution**
- **High depth of investigation**

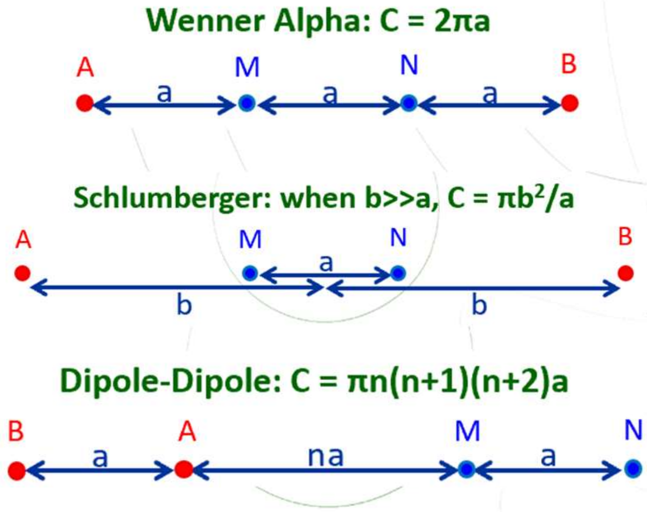

NOTE
Signal strength is inversely proportional to the geometric factor since

$$\Delta V = \frac{\rho_a I}{C}$$

Equipment

Maximum voltage ⇒	1000-2000 *V*
Maximum current ⇒	few Amperes
Electrodes ⇒	metallic

Energy source
- batteries (for brief surveys)
- electrogen group

Generated current
- direct → - survey is affected by self-potentials - electrodes polarize
- switched
- alternating

switched / alternating → - cancel self-potentials - prevent electrode polarization

Voltage measurement ⇒ voltmeter with high input impedance

Electrodes ⇒
- non-polarisable (in case of direct current surveys)
- metallic (in case of switched or alternating current surveys)

Equipment

Traditional equipment (4 electrodes)

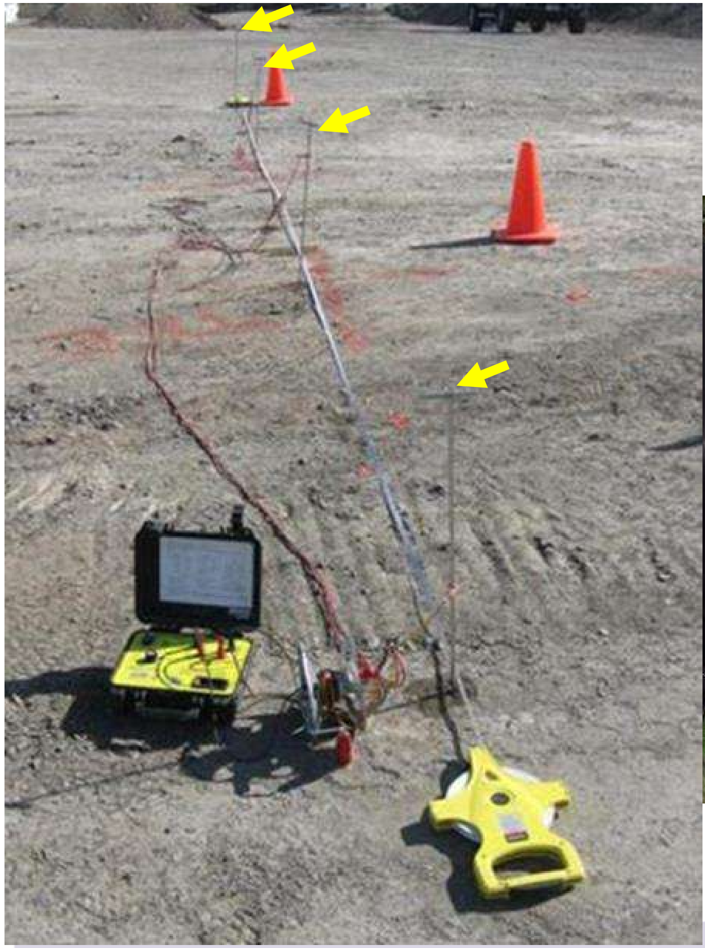

Multielectrode equipment manual switching

Equipment

Multielectrode equipment - automatic switching

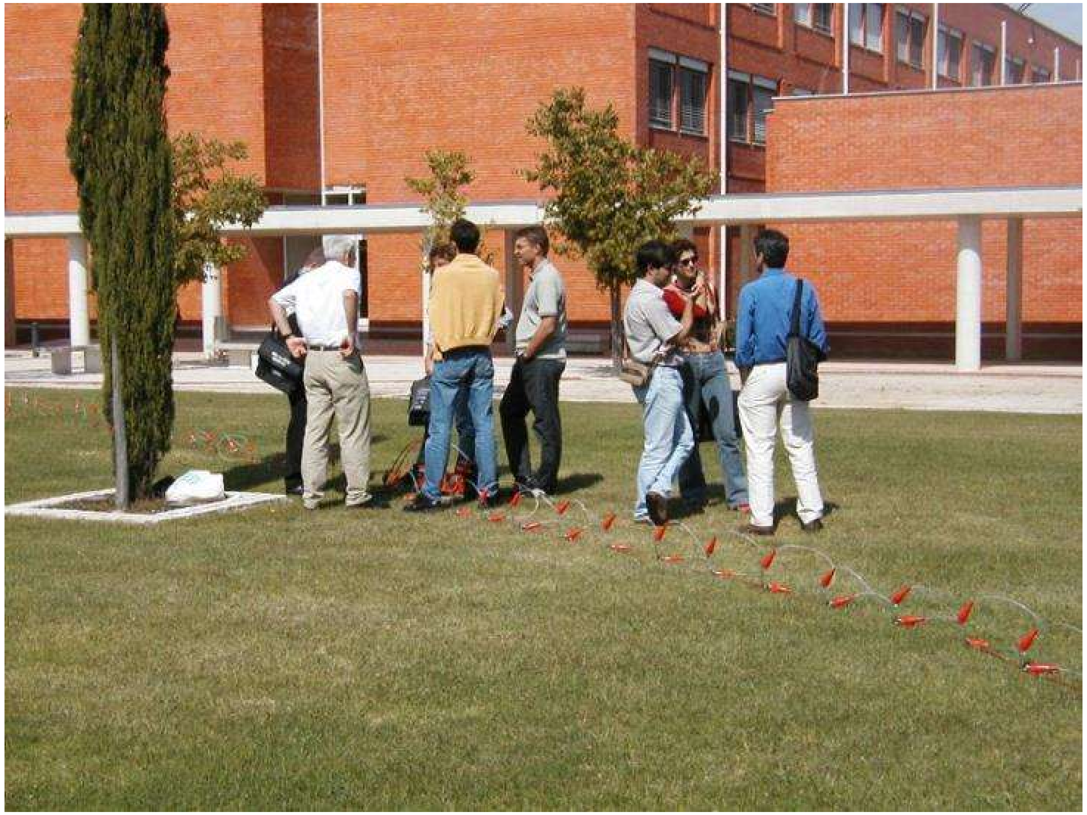

Resistivity measurements - Sounding

In resistivity sounding, mostly known as Vertical Electrical Sounding (VES), the electrode spacing interval is changed while maintaining a fixed location for the center of the electrode spread.

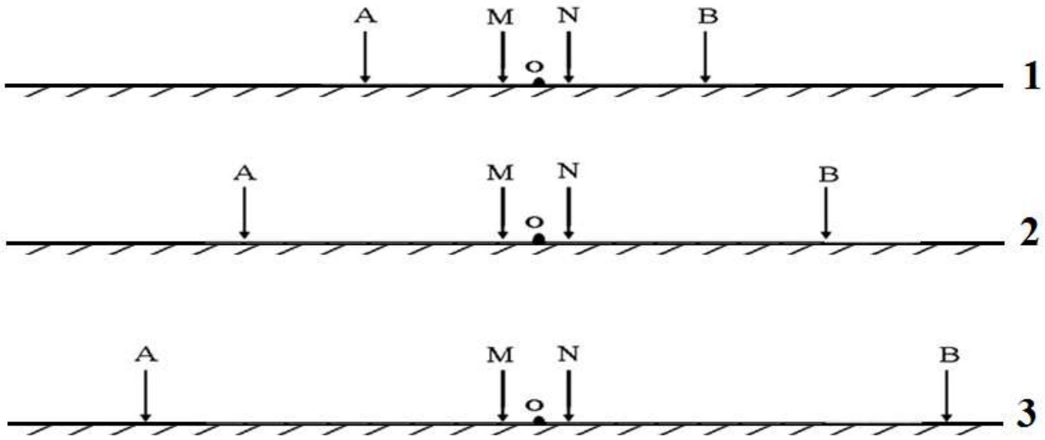

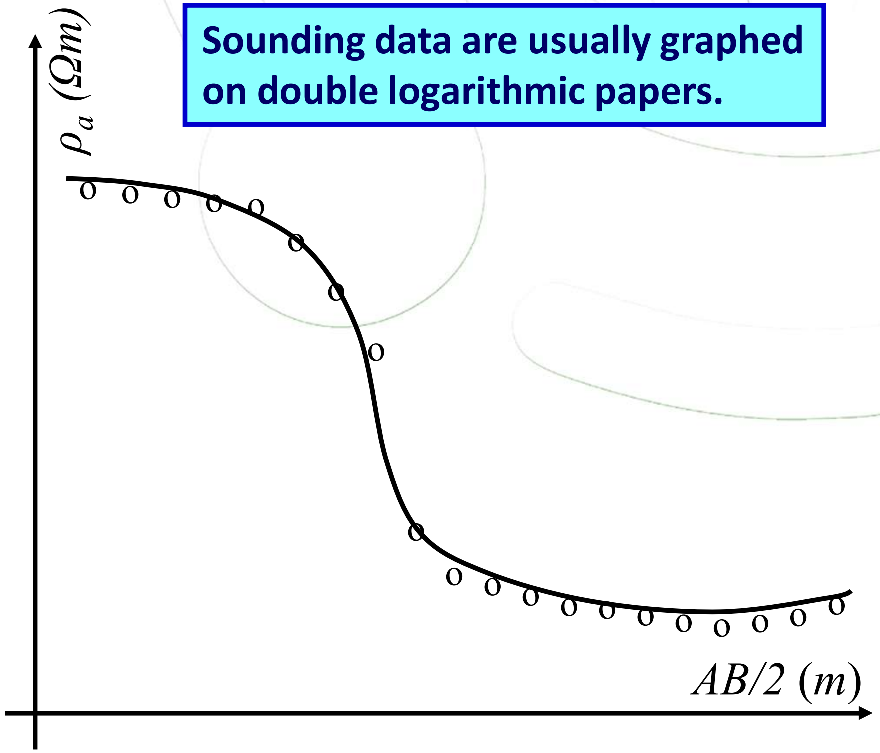

Sounding data are usually graphed on double logarithmic papers.

Resistivity measurements - Profiling

In resistivity profiling surveys, also known as Constant-Separation Traversing (CST), the location of the spread is changed while maintaining a fixed electrode spacing interval.

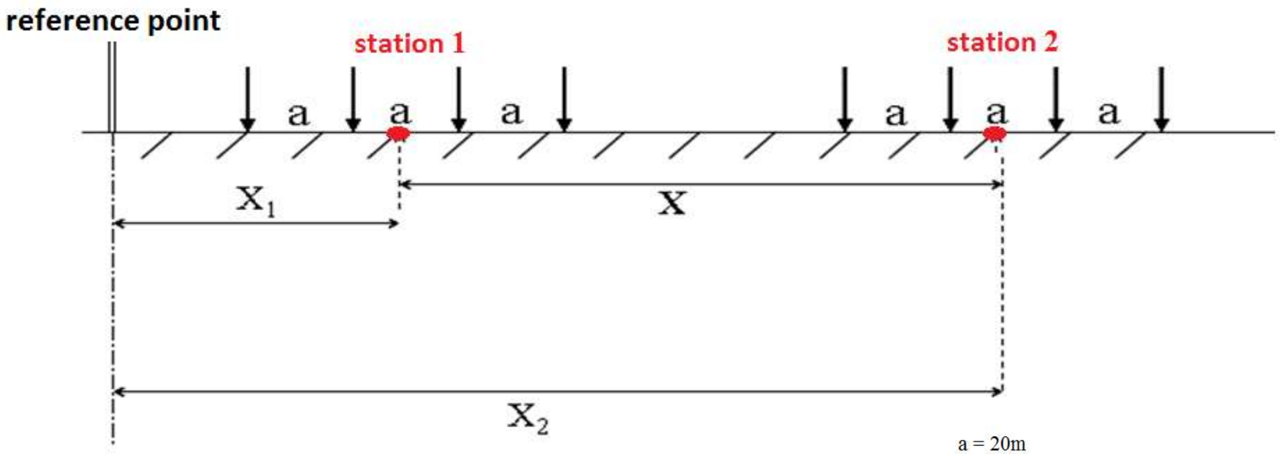

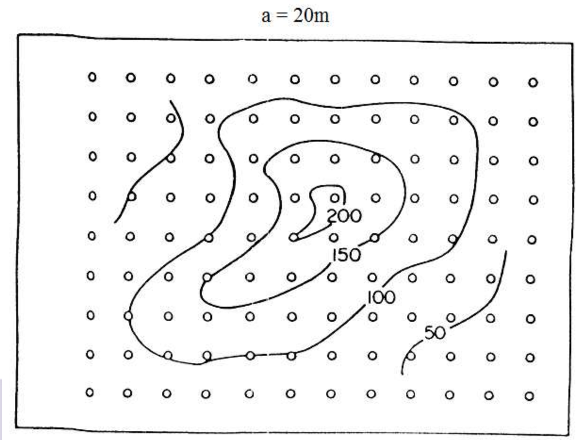

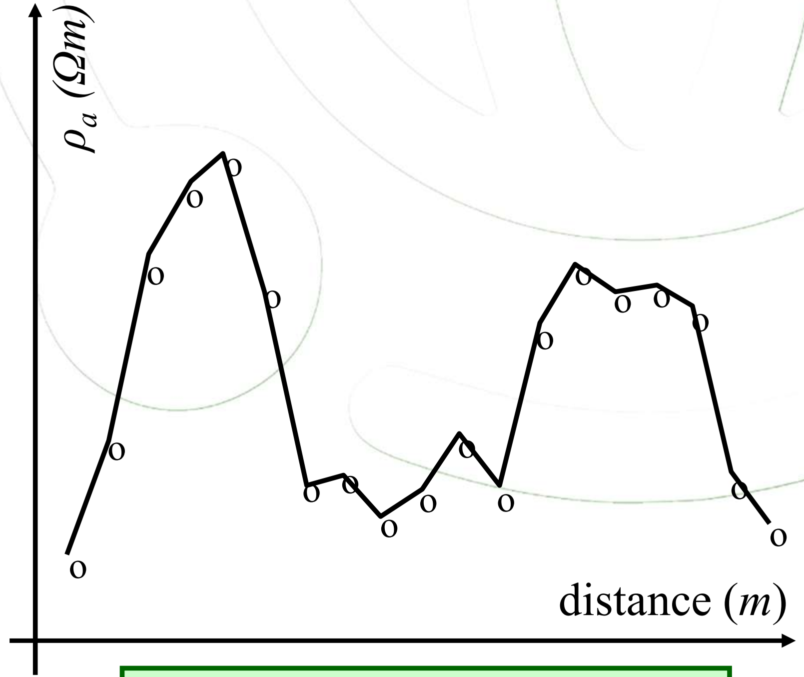

According to field data, a $\rho_a(x)$ diagram is plotted, where x is the position of the central point of the array (*resistivity profile*).

Electrical resistivity tomography (ERT)

Dipole – dipole array

Dipole-dipole array is very sensitive to horizontal changes (but relatively insensitive to vertical changes) in resistivity. Thus it is good in mapping vertical structures, such as dykes and cavities, but relatively poor in mapping horizontal structures such as sedimentary layers.

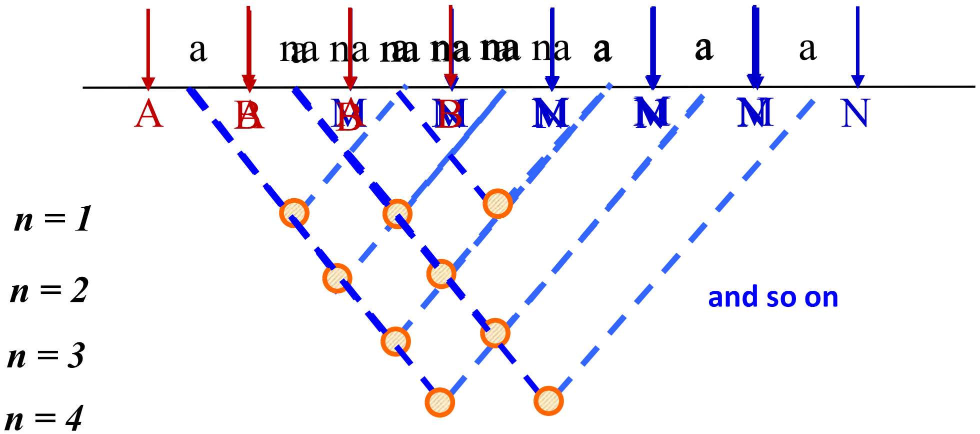

A common mistake is to monotonically increase the "*n*" factor, while keeping the dipole length "*a*" fixed, in an effort to increase the depth of investigation. This usually results in very noisy data.

The "*n*" value should not exceed *6*, and the method of overlapping data levels with different "*a*" dipole lengths can be used

(Loke, 2016)

Electrical resistivity tomography (ERT)

Wenner array

Wenner array is relatively sensitive to vertical changes (and less sensitive to horizontal changes) in the subsurface resistivity below the center of the array. In general, Wenner array is good in resolving vertical changes (i.e. horizontal structures), but relatively poor in detecting horizontal changes (i.e. narrow vertical structures).

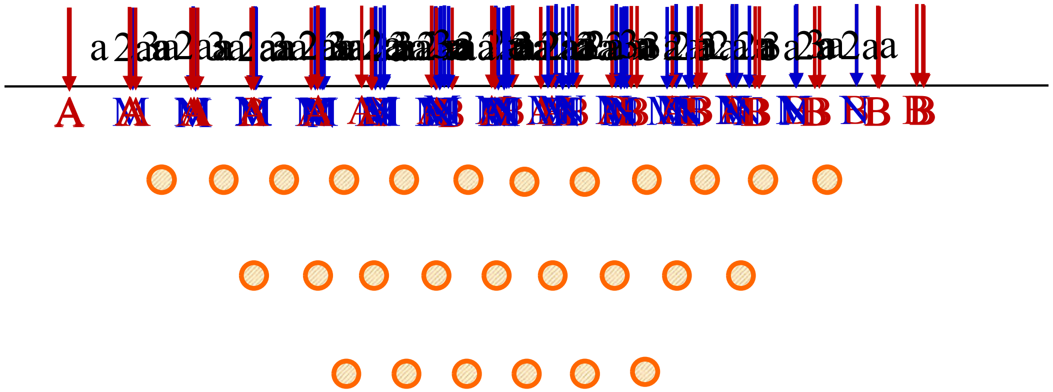

Wenner-Schlumberger array

This is a hybrid between the Wenner and Schlumberger arrays.

In areas where both types of geological structures are expected, this array might be a good compromise between the Wenner and the dipole-dipole array.

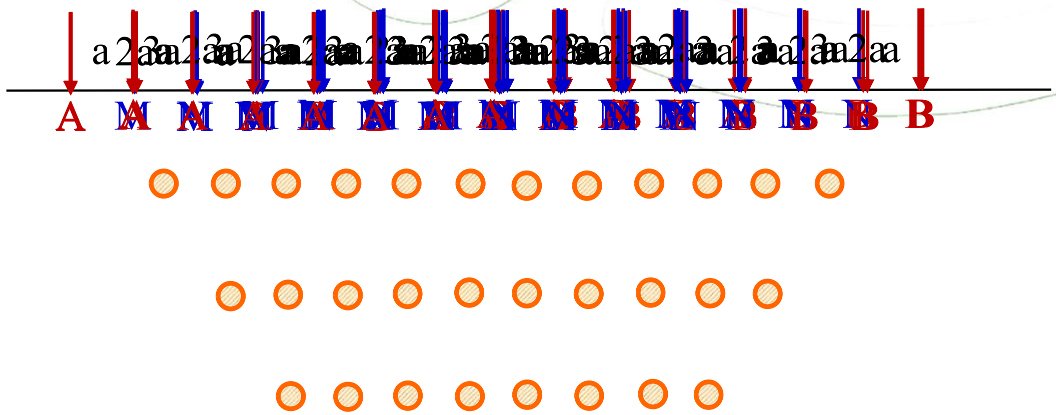

(Loke, 2016)

Electrical resistivity tomography (ERT)

Wenner array

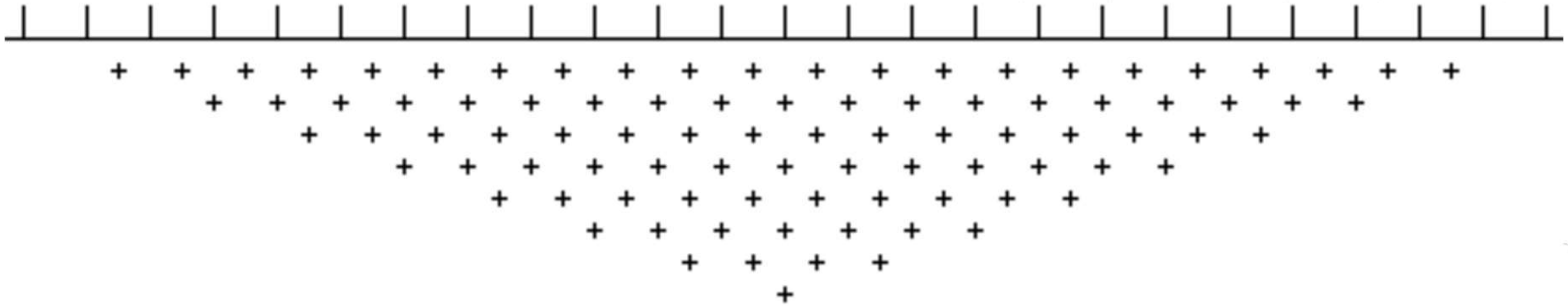

Wenner-Schlumberger array

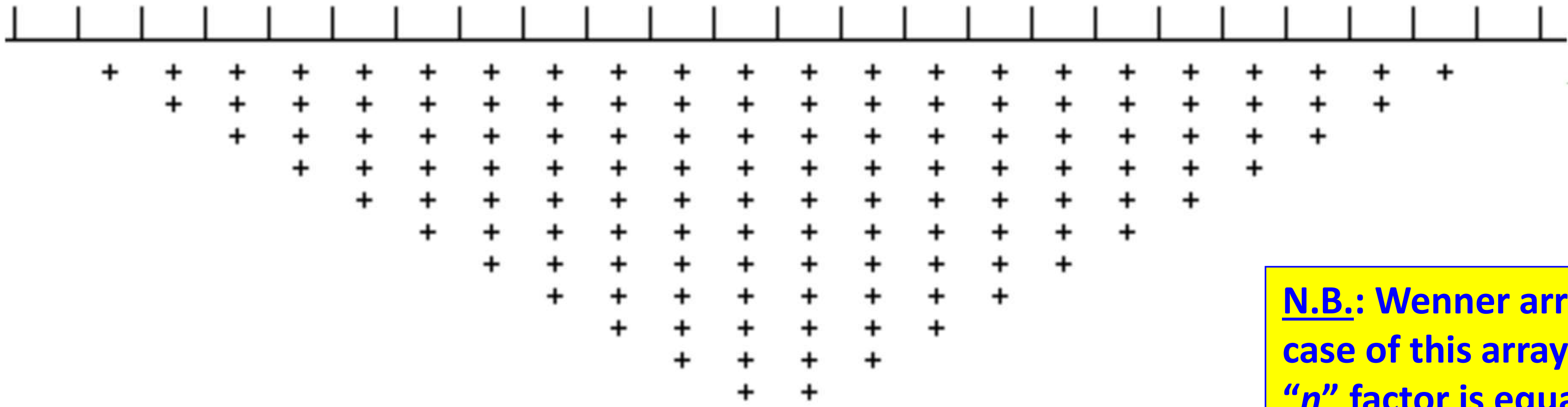

N.B.: Wenner array is a special case of this array where the “*n*” factor is equal to 1.

(Loke, 2016)

Electrical resistivity tomography (ERT)

Data display

Example: Wenner array, a = 2m

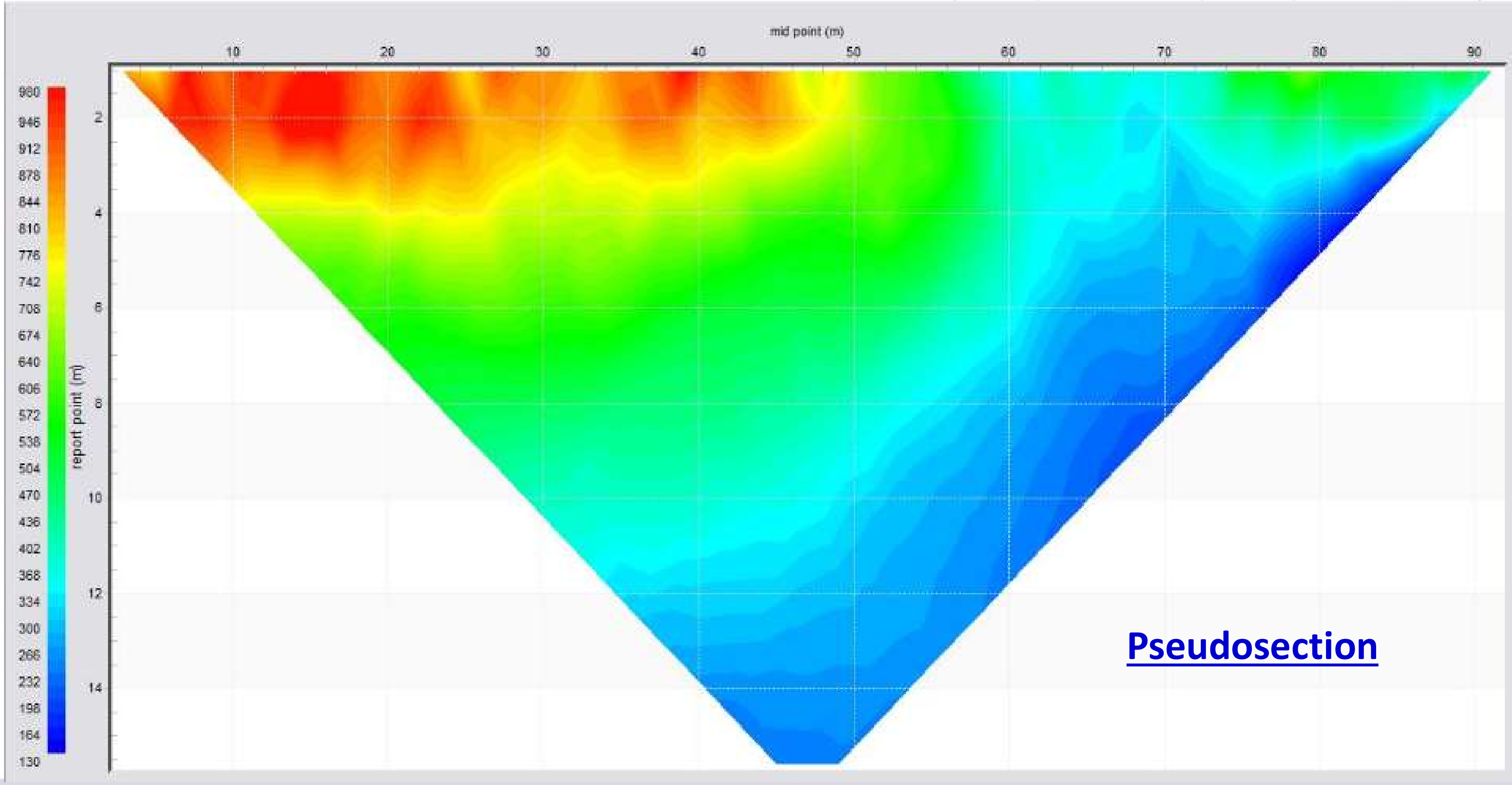

Pseudosection

Interpretation - VES

For resistivity sounding, the available earth models are essentially limited to horizontally layered earth. Each layer is assumed to be uniform.

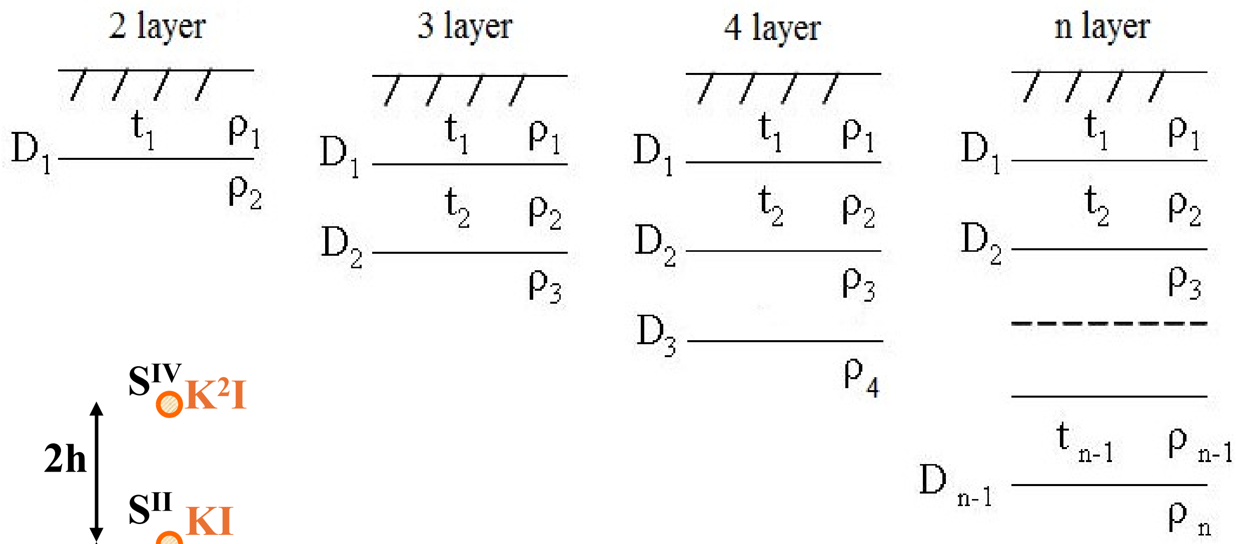

Theoretical models for vertical soundings (2-layer model)

V_P **is the sum of potentials due to** S **and its infinite image sources.**

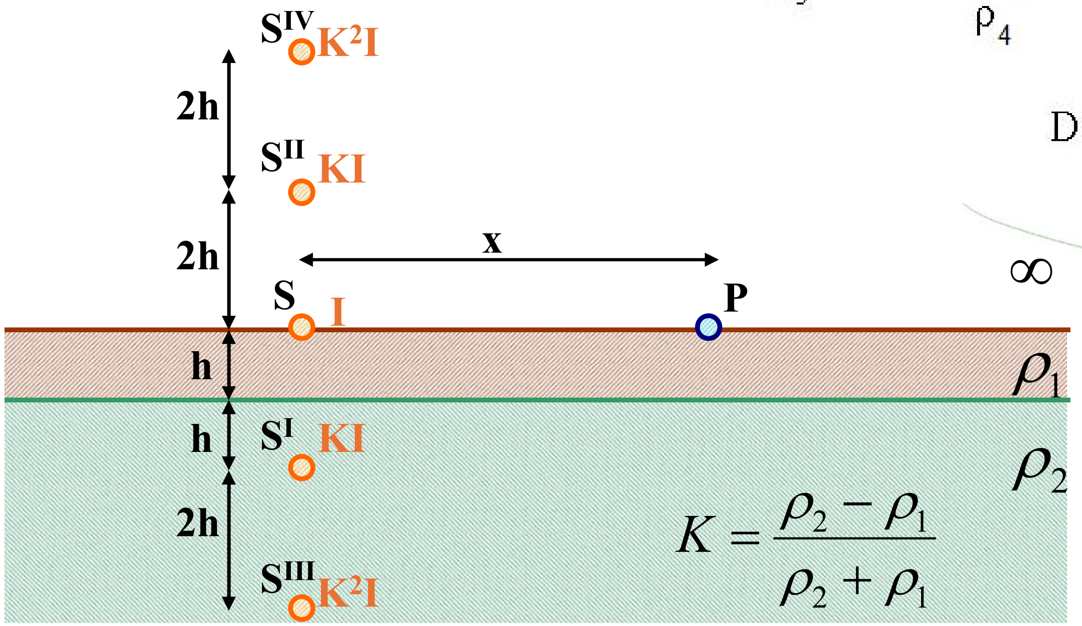

Theoretical models for vertical soundings (2-layer model)

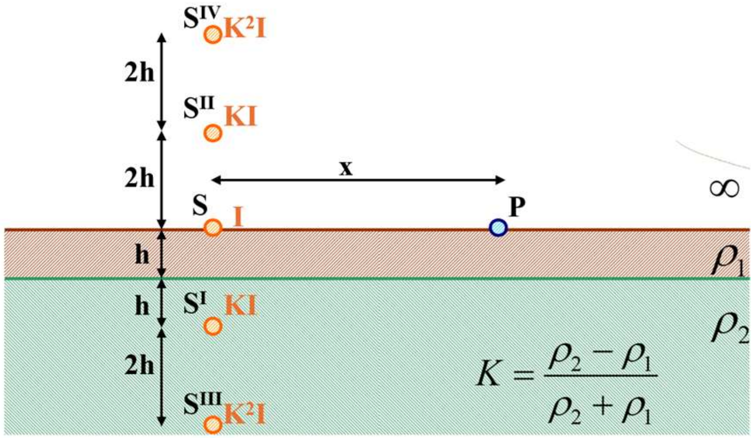

$$K = \frac{\rho_2 - \rho_1}{\rho_2 + \rho_1}$$

$$V_P = \frac{\rho_1 I}{2\pi}\left(\frac{1}{x} + 2\frac{k}{\sqrt{x^2 + (2h)^2}} + 2\frac{k^2}{\sqrt{x^2 + (4h)^2}} + \ldots\right) =$$

$$V_P = \frac{\rho_1 I}{2\pi}\left(\frac{1}{x} + 2\sum_{n=1}^{\infty}\frac{k^n}{\sqrt{x^2 + (2nh)^2}}\right)$$

Using Wenner configuration: $\Delta V = V_M(A) + V_M(B) - V_N(A) - V_N(B) = 2V_M(A) - 2V_N(A)$

$$\Delta V = \frac{\rho_1 I}{2\pi} 2\left[\left(\frac{1}{a} + 2\sum_{n=1}^{\infty}\frac{k^n}{\sqrt{a^2 + (2nh)^2}}\right) - \left(\frac{1}{2a} + 2\sum_{n=1}^{\infty}\frac{k^n}{\sqrt{4a^2 + (2nh)^2}}\right)\right]$$

$$\Delta V = \frac{\rho_1 I}{2\pi}\left(\frac{1}{a} + 4\sum_{n=1}^{\infty}\frac{k^n}{\sqrt{a^2 + (2nh)^2}} - 4\sum_{n=1}^{\infty}\frac{k^n}{\sqrt{4a^2 + (2nh)^2}}\right)$$

Theoretical models for vertical soundings (2-layer model)

$$\rho_a = \frac{\Delta V}{I} 2\pi a = \rho_1 \left(1 + 4\sum_{n=1}^{\infty} \frac{k^n}{\sqrt{1+\left(2n\frac{h}{a}\right)^2}} - 4\sum_{n=1}^{\infty} \frac{k^n}{\sqrt{4+\left(2n\frac{h}{a}\right)^2}} \right)$$

$$\text{when } \frac{h}{a} \to \infty \;\Rightarrow\; \rho_a \to \rho_1$$

$$\text{when } \frac{h}{a} \to 0 \;\Rightarrow\; \rho_a = \rho_1 \left(1 + 4\sum_{n=1}^{\infty} k^n - 4\sum_{n=1}^{\infty} \frac{k^n}{2} \right) = \rho_1 \left(1 + 2\sum_{n=1}^{\infty} k^n \right) =$$

$$= \rho_1 \left[1 + 2\left(\frac{1}{1-k} - 1 \right) \right] = \rho_1 \frac{1+k}{1-k} = \rho_2$$

Theoretical models for vertical soundings (2-layer model)

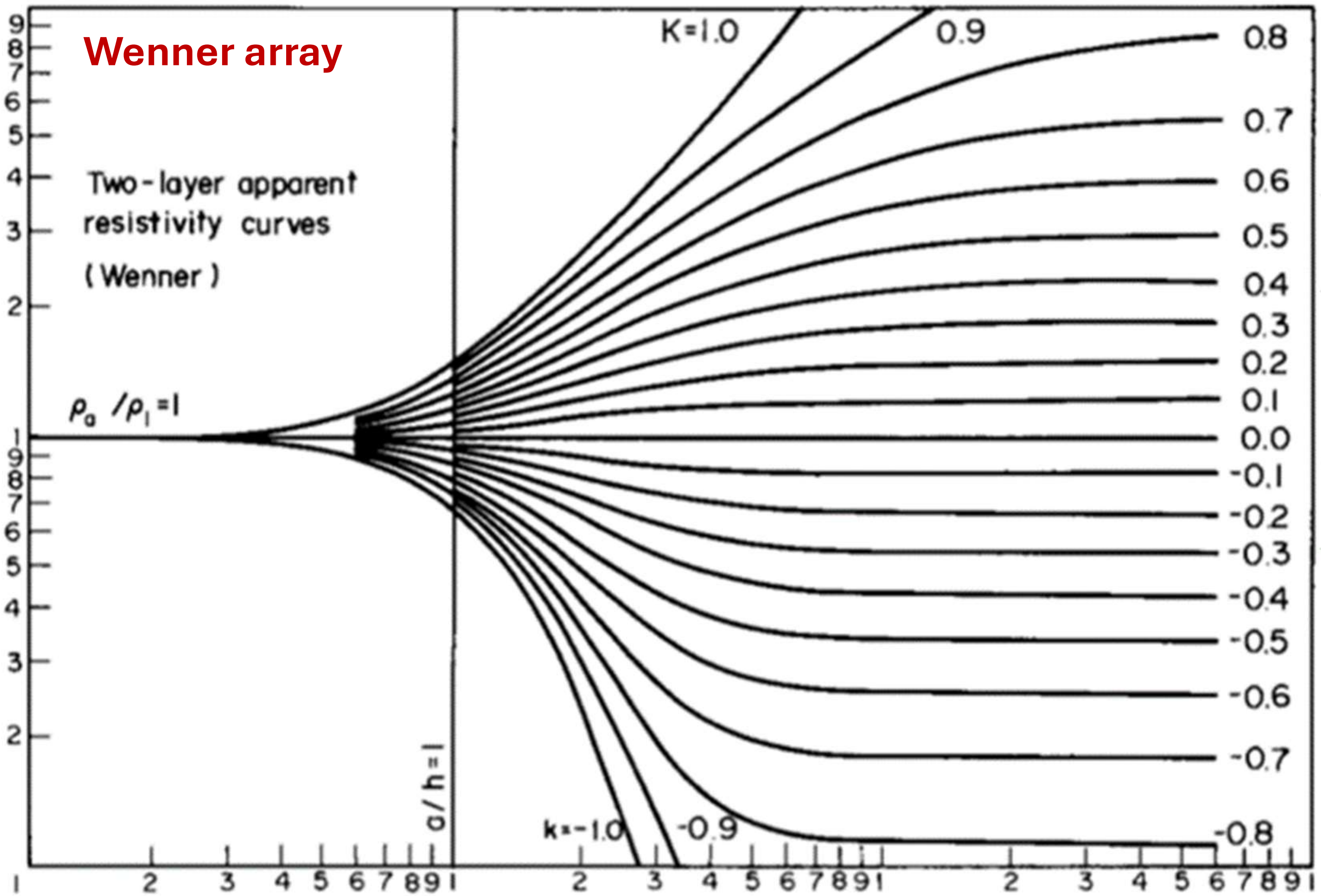

Interpretation - VES

ITINERIS

Curve matching

1- Plotting the field resistivity curve (smoothed and corrected as necessary) on a transparent log–log paper with the same scale as the master curves.

2- Placing the field curve on the appropriate set of master curves and, keeping the two sets of axes parallel, moving the field curve about until a fit is obtained, or until it appears to be interpolated between adjacent curves in the correct place.

3- Now, the $\rho_a/\rho_1=1$ and the $a/z=1$ axes of the master curves respectively cut the ordinate and the abscissa of the field curve at $\rho_a=\rho_1$ and $a=z$.

4- The reflection coefficient of the field curve (to calculate ρ_2) is that of the best–fitting master curve.

Interpretation - Profiling

Different types of anomaly is produced depending on the electrode configuration and whether it is developed at right angles or parallel to the boundary.

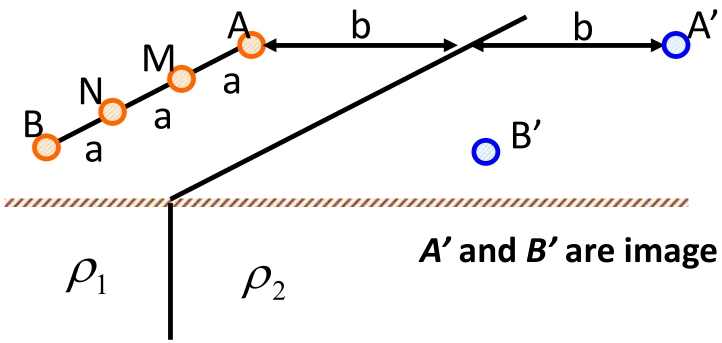

A' **and** ***B'*** **are image sources**

$$K = \frac{\rho_2 - \rho_1}{\rho_2 + \rho_1}$$

Plan view

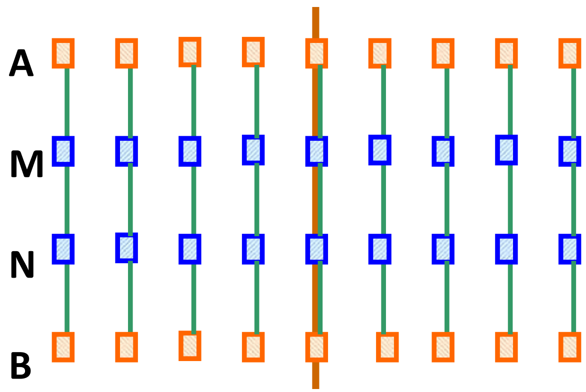

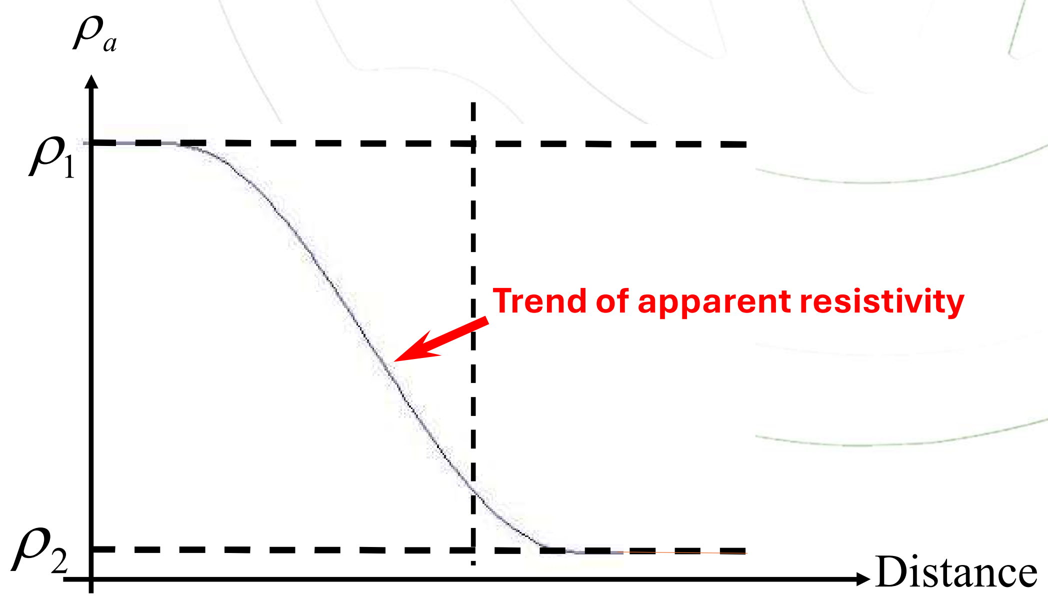

Interpretation - Profiling

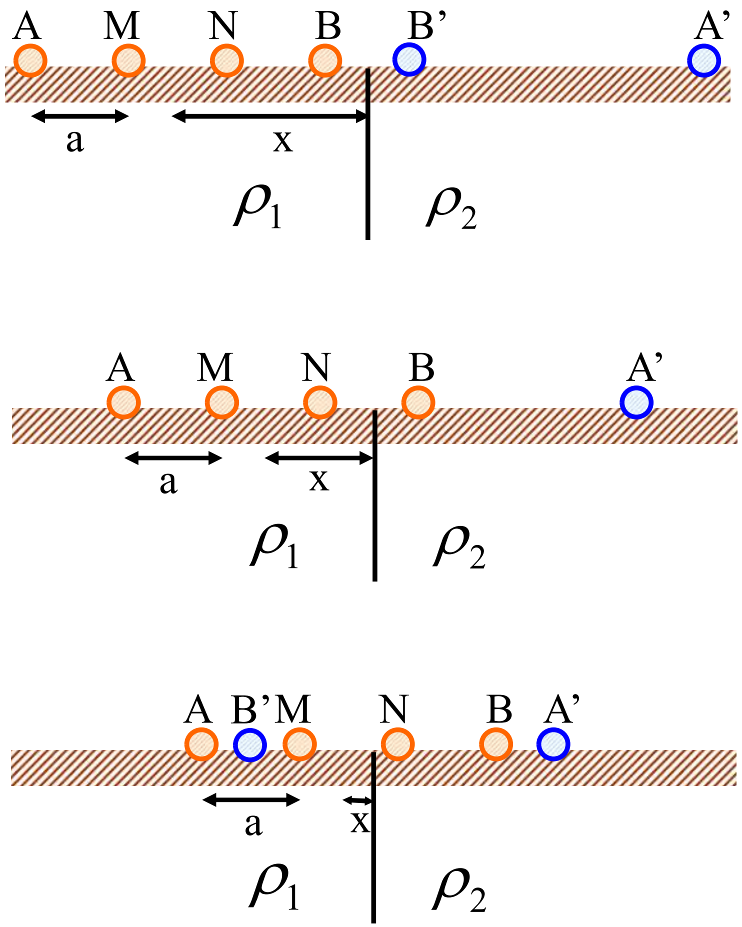

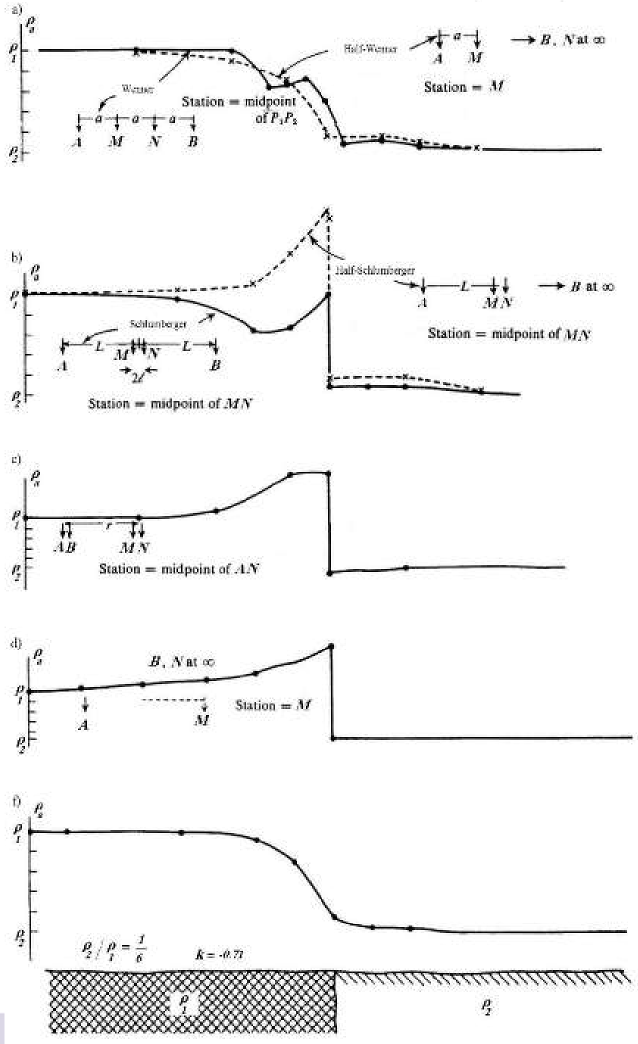

(Telford et al., 1990)

All five possible situations depending on electrode positions with respect to the contact.

Plan view

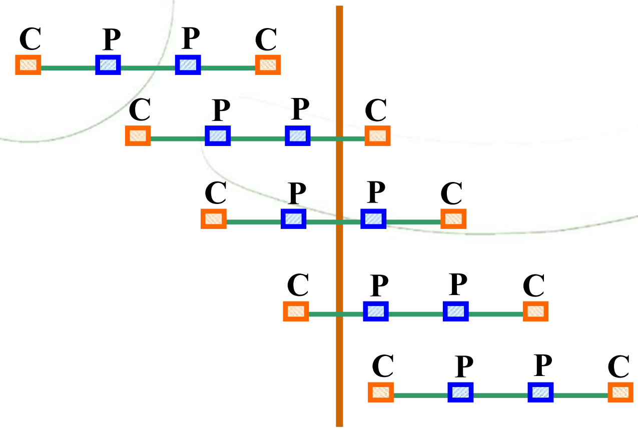

C = current electrodes
P = potential electrodes

Interpretation - ERT

Iterative inversion methods

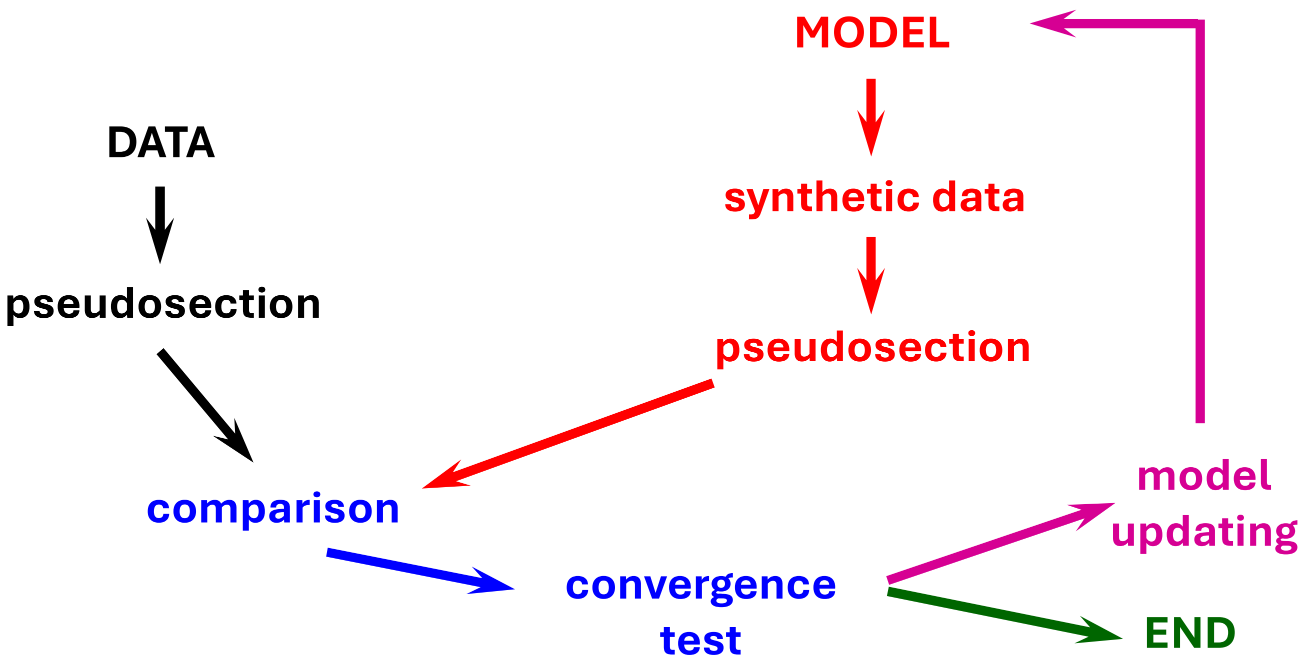

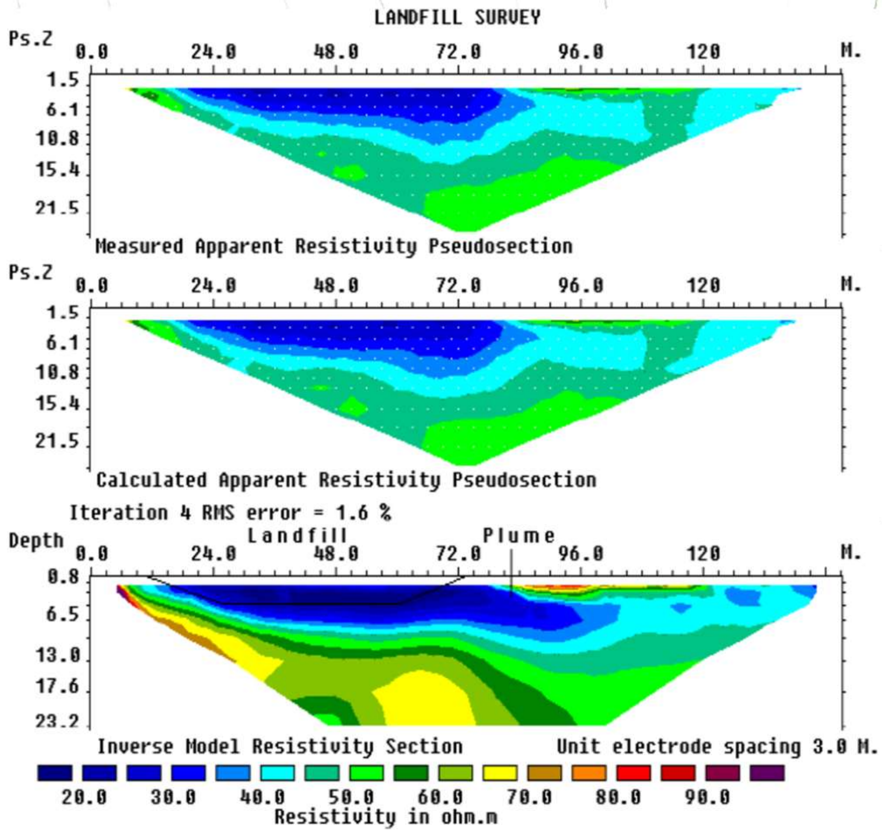

(Loke, 2016)

Applications

Civil engineering: thickness and saturation level of sediments, depth to bedrock, locations of subsurface cavities (natural or manmade)

Archeological investigations: location of buried foundations, walls, roads, tunnels

Hydrogeological studies: groundwater, saltwater intrusion into freshwater aquifers

Environmental investigations:
evaluation of contamination level,
mapping pollutant diffusion,
assessment of abandoned landfill areas

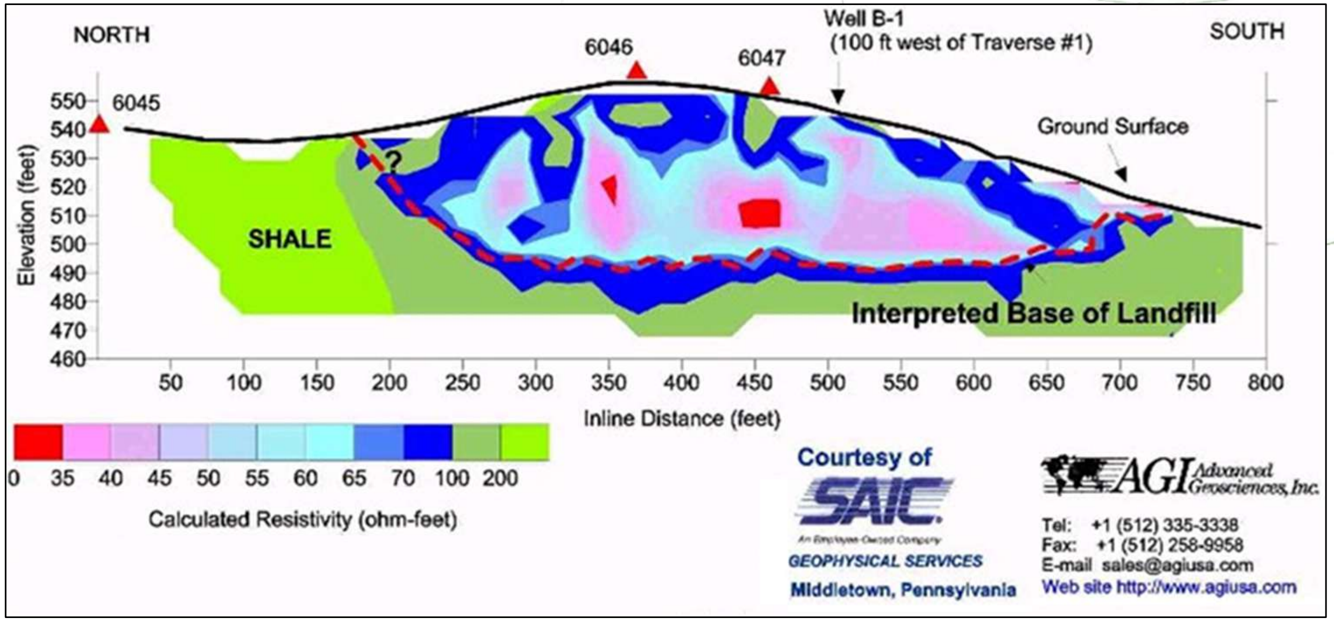

Examples: cavity

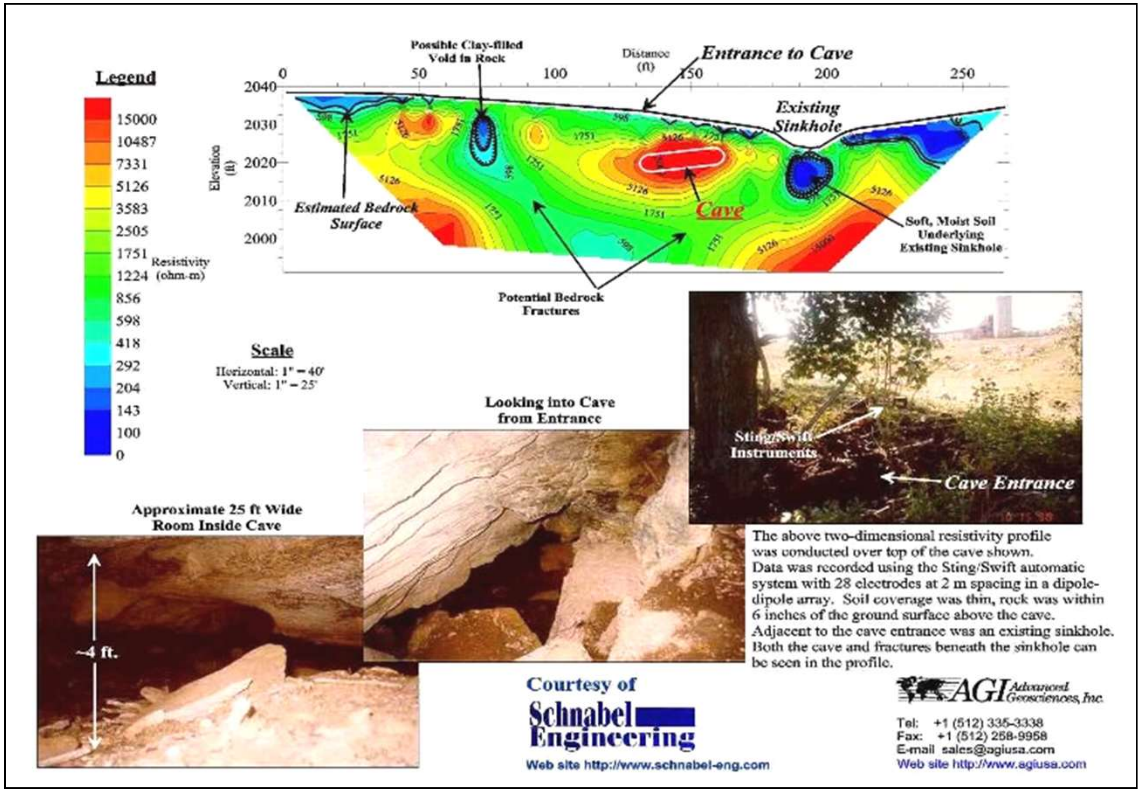

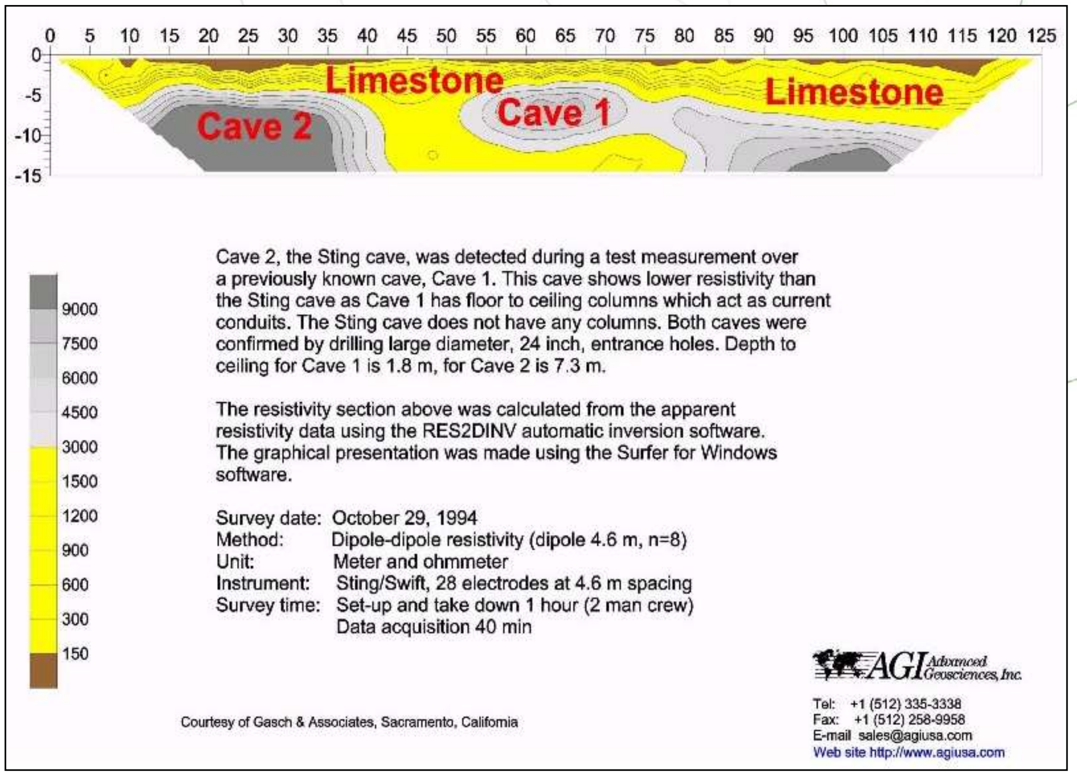

Example: qanat

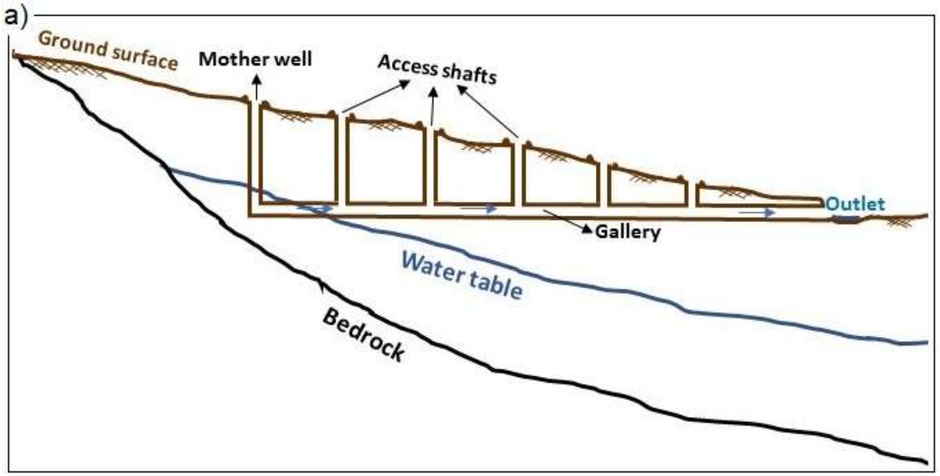

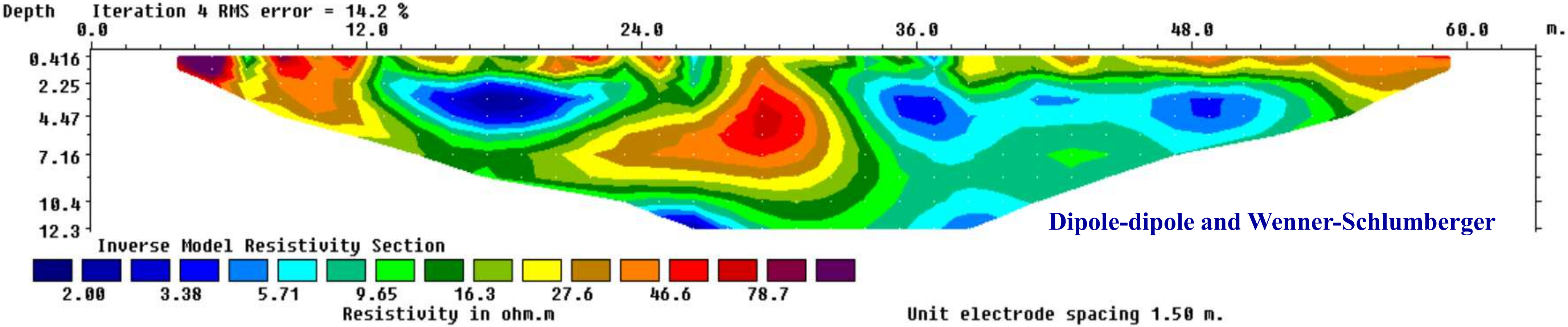

(Hojat et al., 2016, 2023)

Example: qanat

Hosting material: sand | **Hosting material: clay**

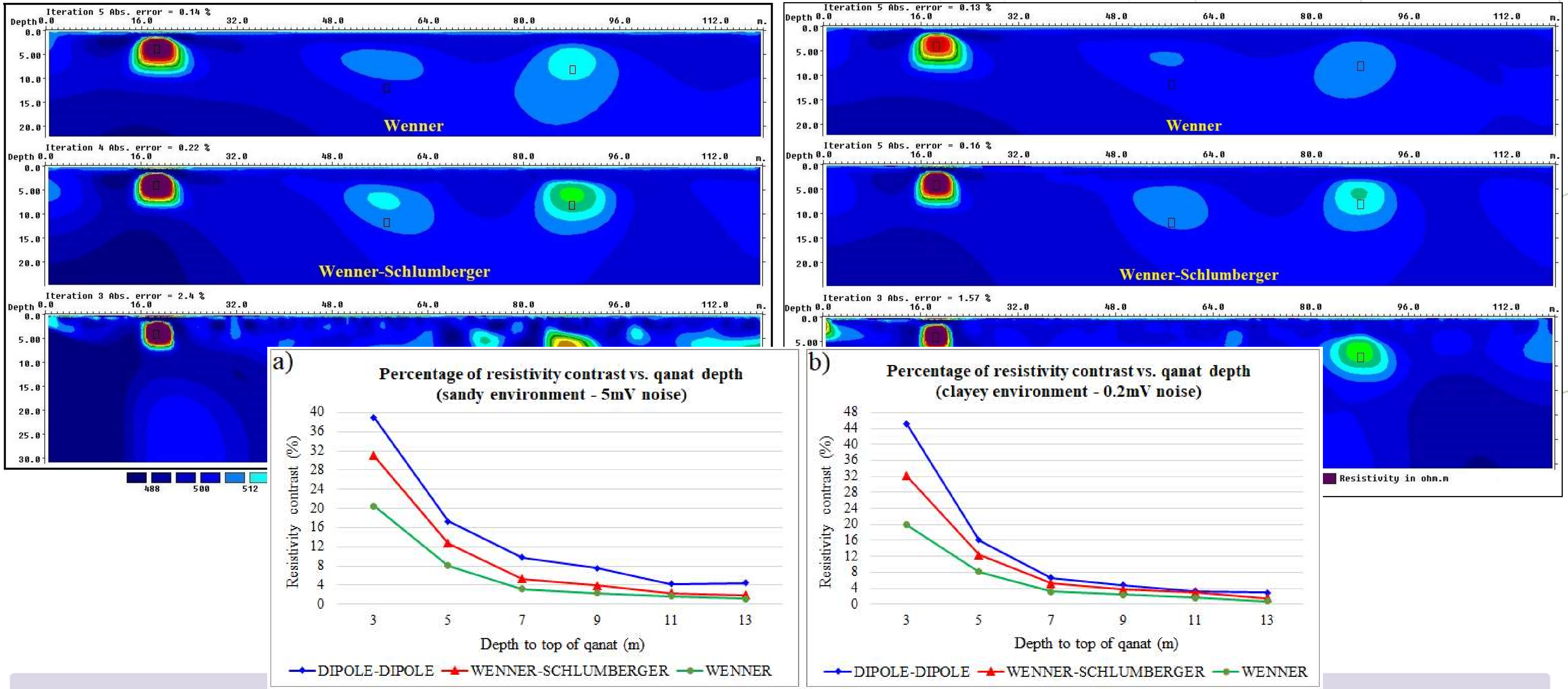

(Hojat et al., 2021)

Example: pore fluids

Aim: **Exploring the feasibility of ERT surveys to detect acid saturated zones in a copper heap leaching site**

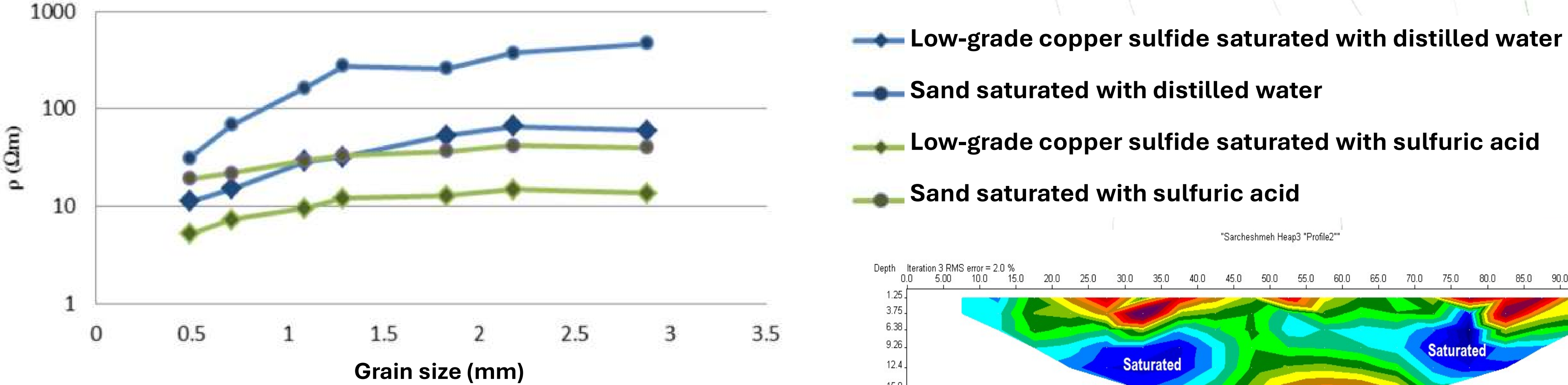

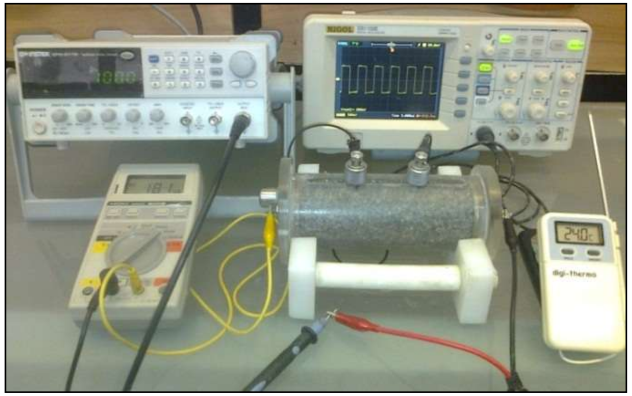

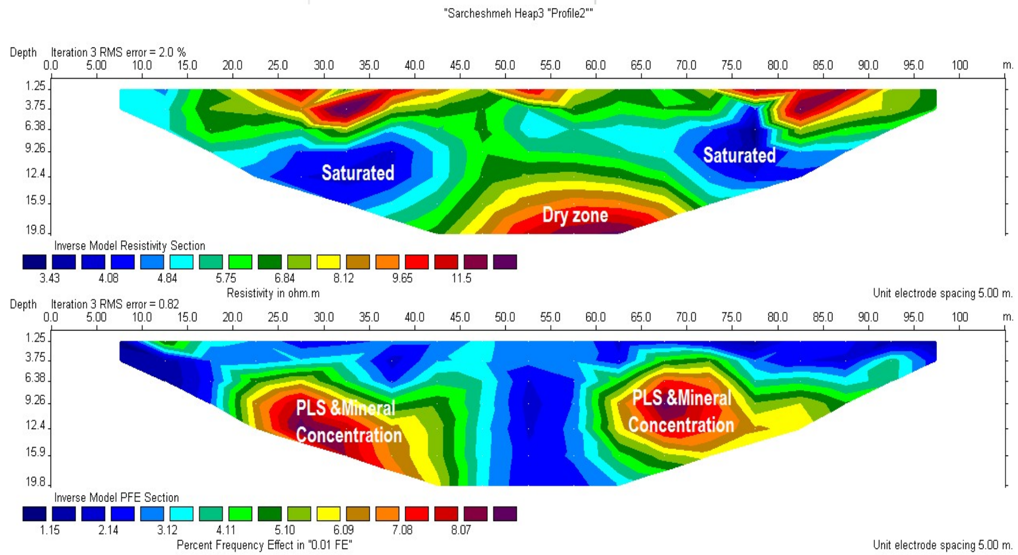

(Moradipour et al., 2015, 2016)

Example: tunnel investigations

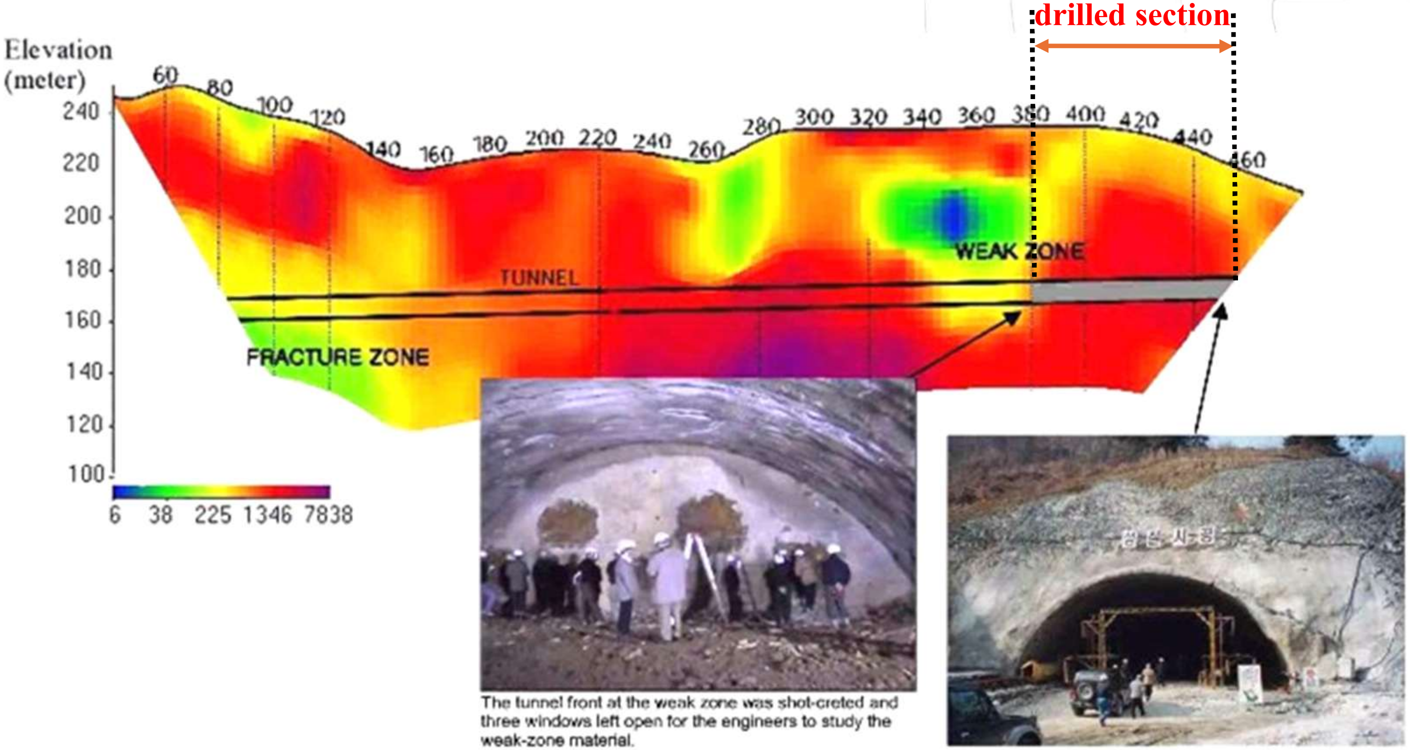

The tunnel front at the weak zone was shot-creted and three windows left open for the engineers to study the weak-zone material.

The entrance to one of the two parallel tunnels

Objective:	Site investigation for two parallel highway tunnels. The weak zone between 340-380 meter was confirmed during the actual tunnel construction and consisted of fractured limestone and soft moist clay.
Survey site:	South of Seoul, Korea
Method:	Dipole-dipole resistivity
Instrument:	Sting/Swift, 27 electrodes at 20 meter spacing
Processing:	Inversion using the DIPRO software
Units:	Meter and ohmmeter

AGI Advanced Geosciences, Inc.

Tel: +1 (512) 335-3338
Fax: +1 (512) 258-9958
E-mail sales@agiusa.com
Web site http://www.agiusa.com

Courtesy of Hyundai Institute of Construction Technology

Example: monitoring of river levees

Location: San Giacomo delle Segnate (MN)

1. **Via Marconi**
2. **Via Dugale**

Aims: Time-lapse resistivity measurements to monitor the conditions of river levees.

(Tresoldi, 2016)

Example: monitoring of river levees

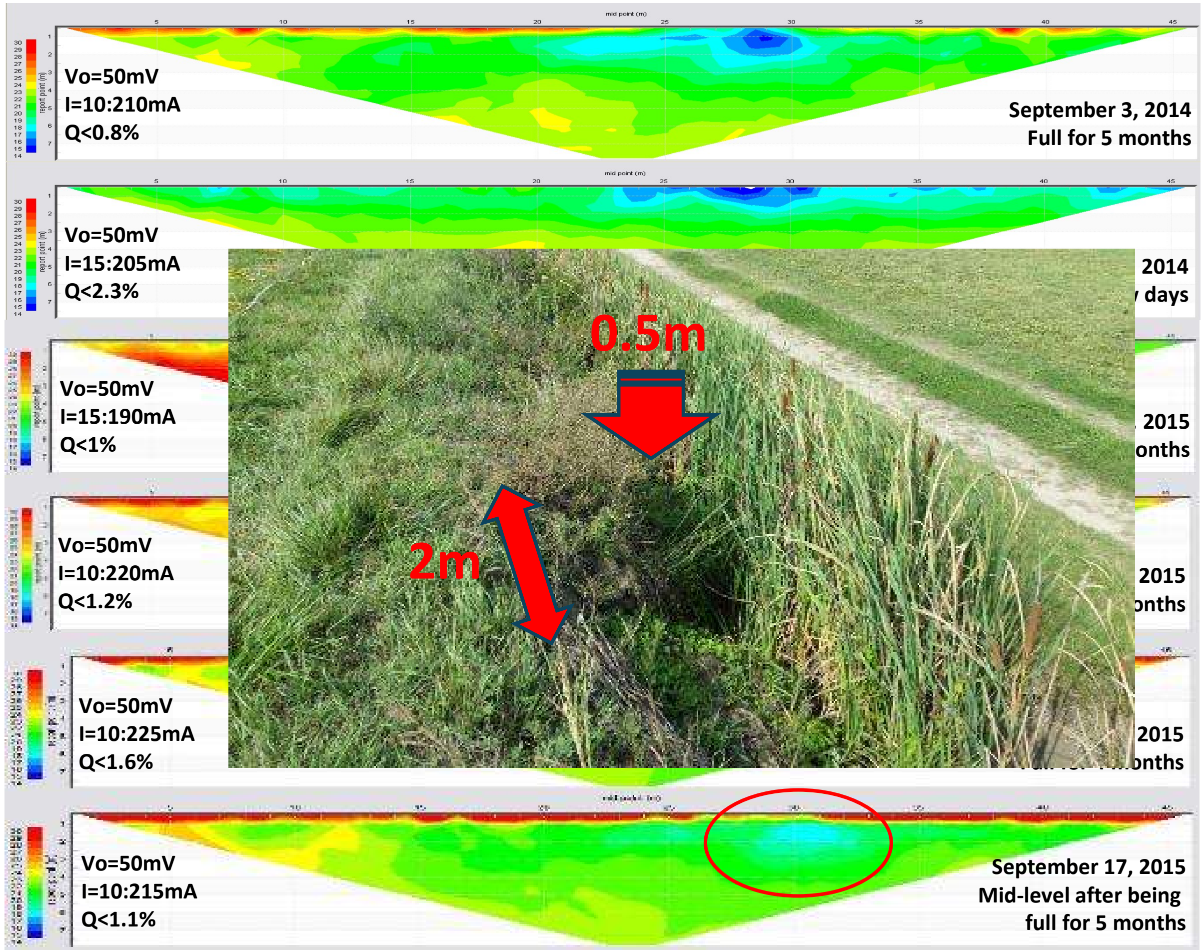

(Tresoldi, 2016)

Example: monitoring of river levees

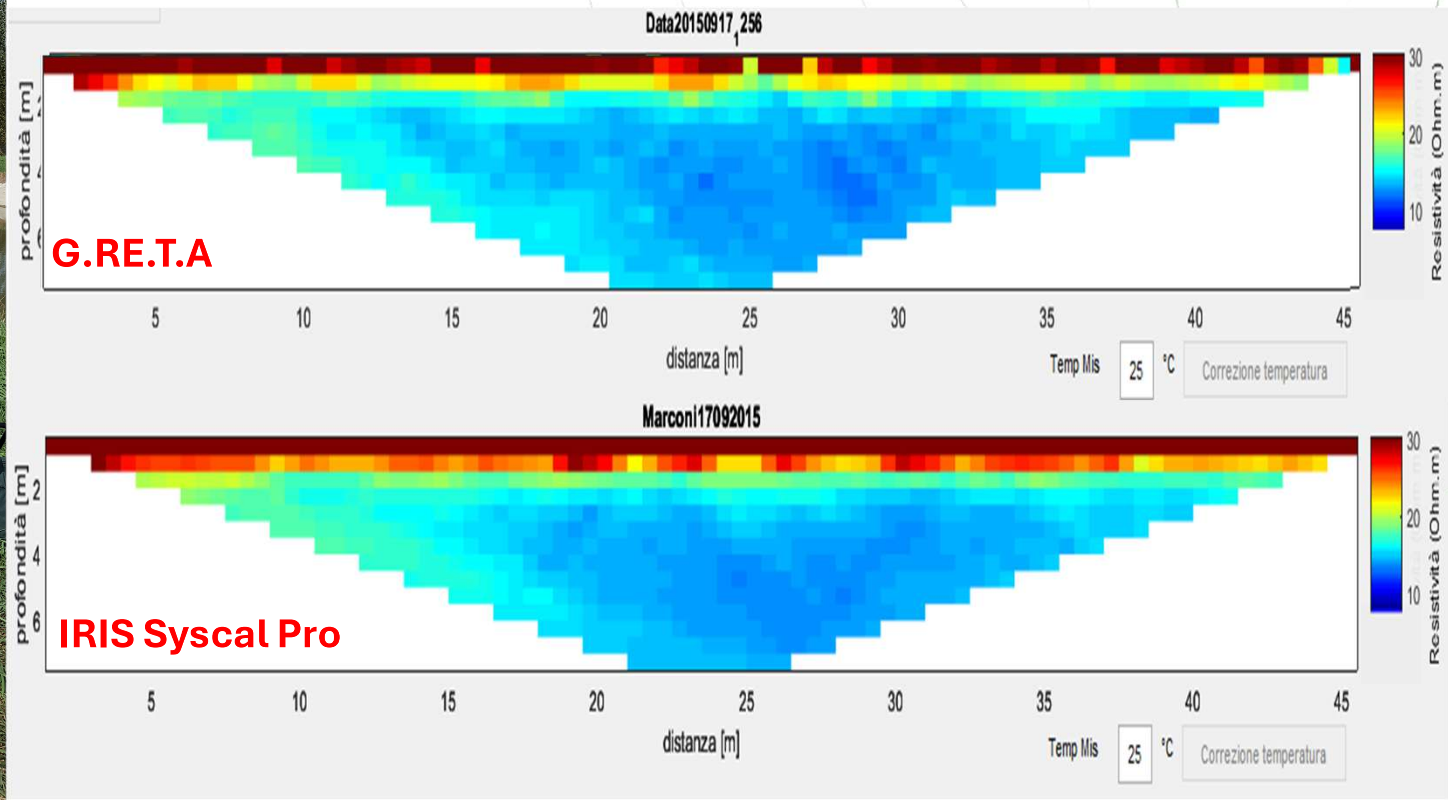

Example: monitoring of river levees

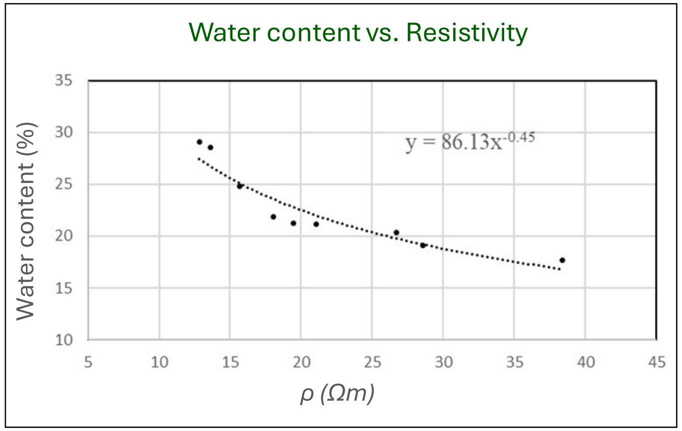

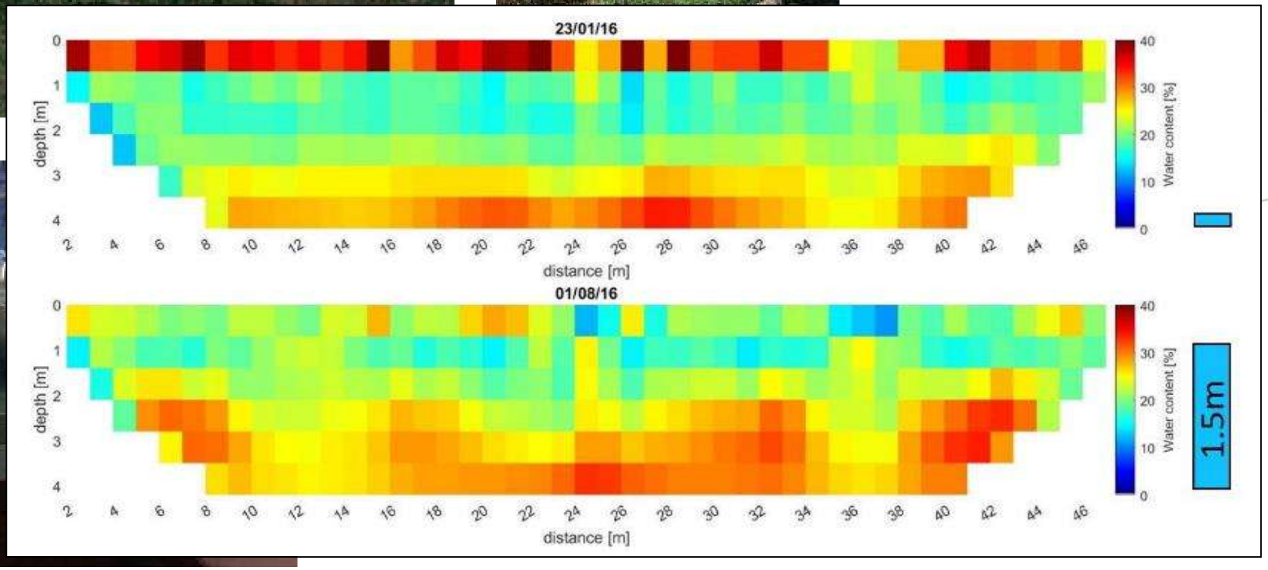

Example: monitoring of river levees

Location: Colorno, Parma

Aim: Time-lapse resistivity measurements to monitor the most critical section of Parma river embankment

Colorno, Parma (December 2017)

Example: monitoring of river levees

ITINERIS

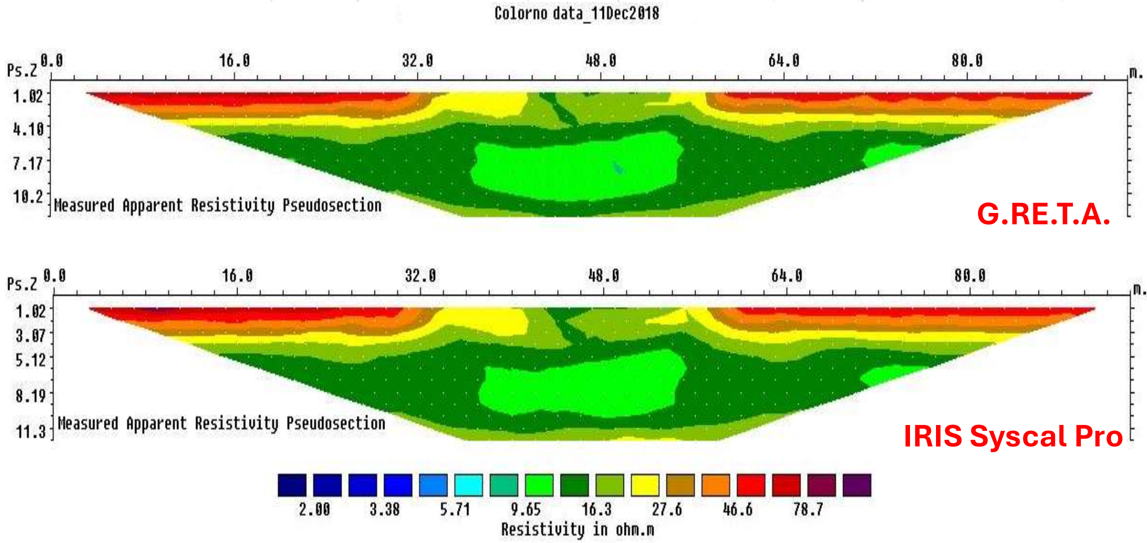

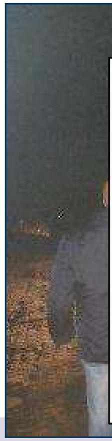

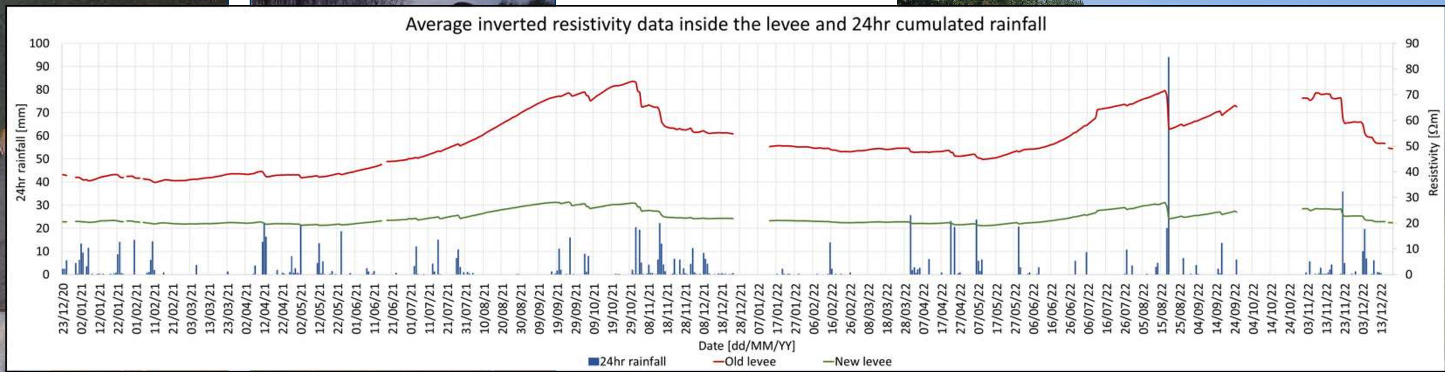

(Hojat et al., 2019; Bianchi et al. 2024)

Example: monitoring of critical slopes

Location: Madonna del Piano

Aim: Time-lapse resistivity measurements to monitor the water table fluctuations

Example: monitoring of critical slopes

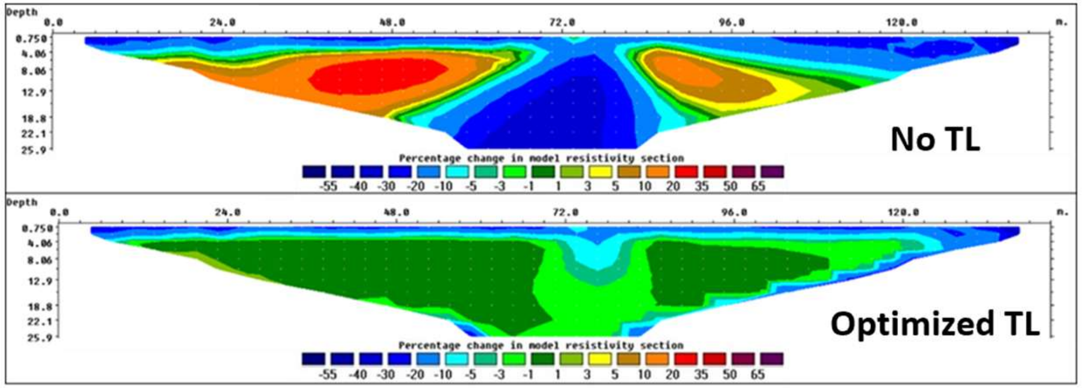

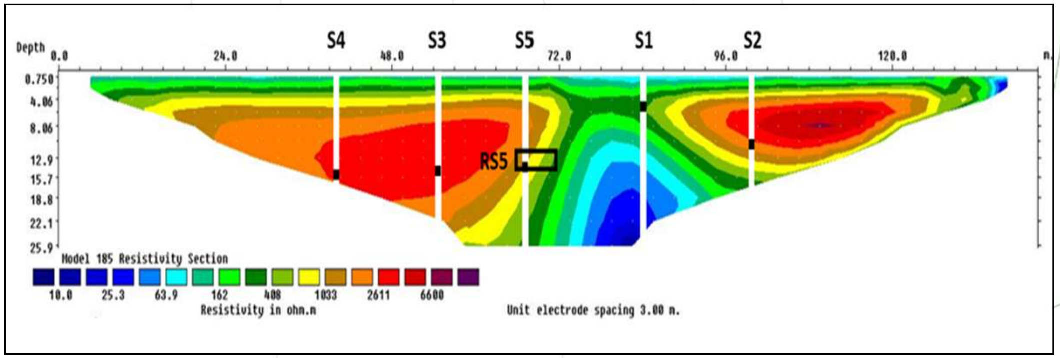

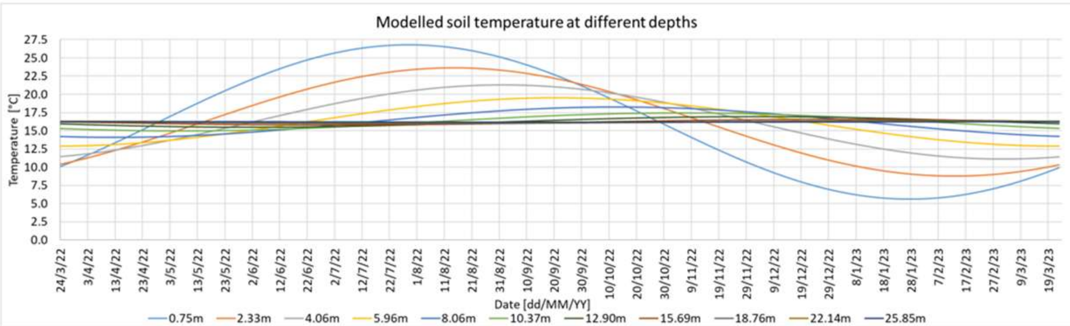

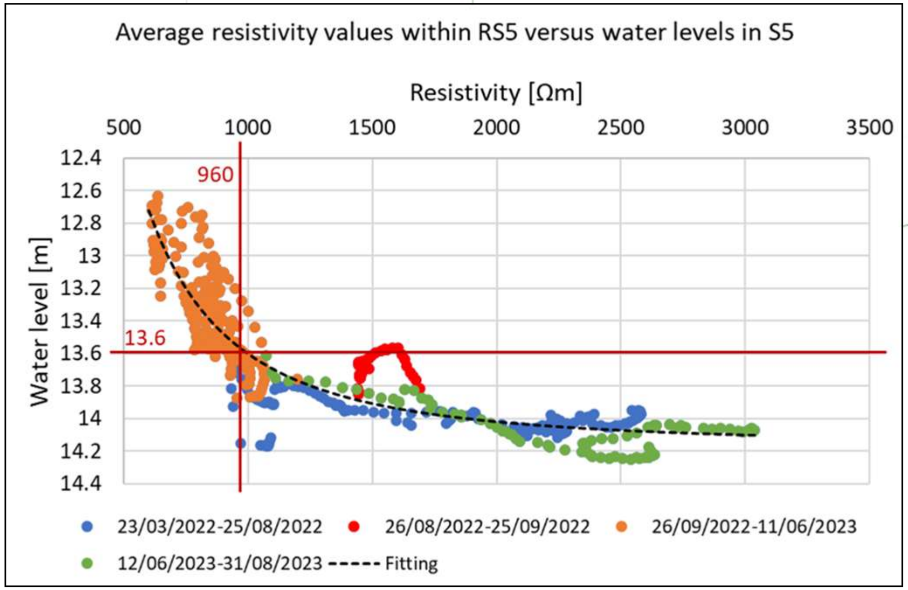

Interpretation challenges: buried electrodes

Tests performed on the size and type of electrodes to keep contact resistances low.

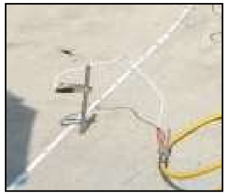

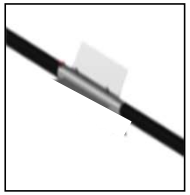
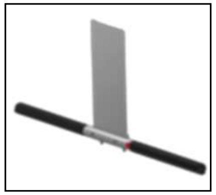

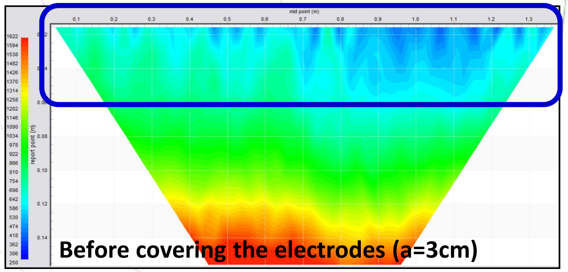

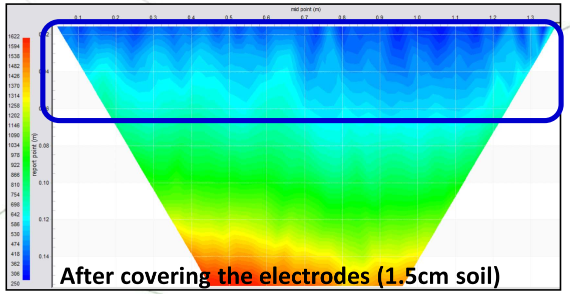

Apparent resistivity calculation for buried electrodes?

$$\rho_a = C\frac{\Delta V}{I}$$

Surface electrodes:

$$C = \frac{2\pi}{\left\{\left(\frac{1}{r_{AM}} - \frac{1}{r_{BM}}\right) - \left(\frac{1}{r_{AN}} - \frac{1}{r_{BN}}\right)\right\}}$$

Buried electrodes:

$$C = \frac{4\pi}{\left\{\left(\frac{1}{r_{AM}} - \frac{1}{r_{BM}}\right) - \left(\frac{1}{r_{AN}} - \frac{1}{r_{BN}}\right) + \left(\frac{1}{r_{A'M}} - \frac{1}{r_{B'M}}\right) - \left(\frac{1}{r_{A'N}} - \frac{1}{r_{B'N}}\right)\right\}}$$

A and B: current electrodes; M and N: potential electrodes
r: distance between electrodes
A' and B': current images above the ground surface for buried electrodes

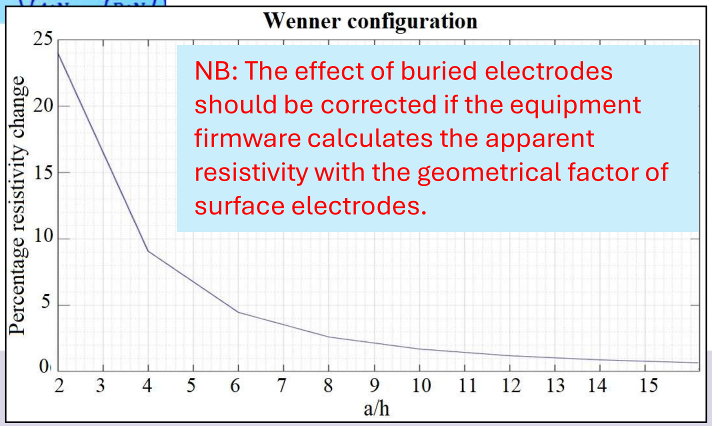

Interpretation challenges: 3D effects

The apparent resistivity measurements are affected not only by materials directly below the line, but also by resistivity changes perpendicular to ERT profile (Water and air on one side, and air on the other side).

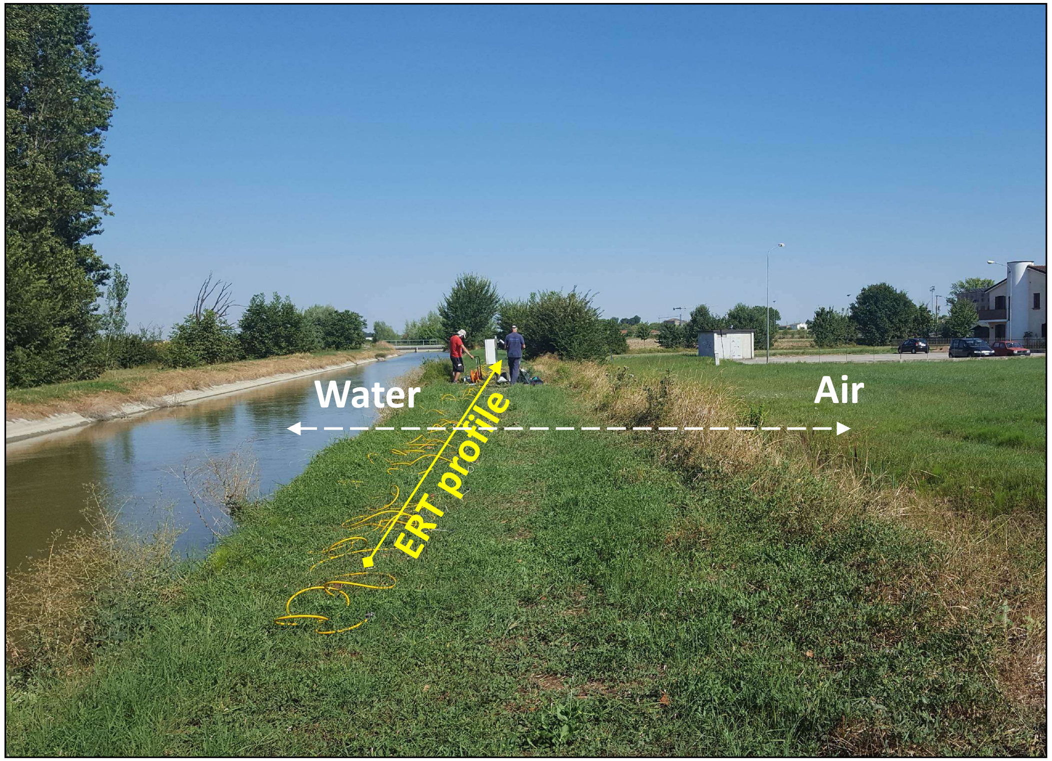

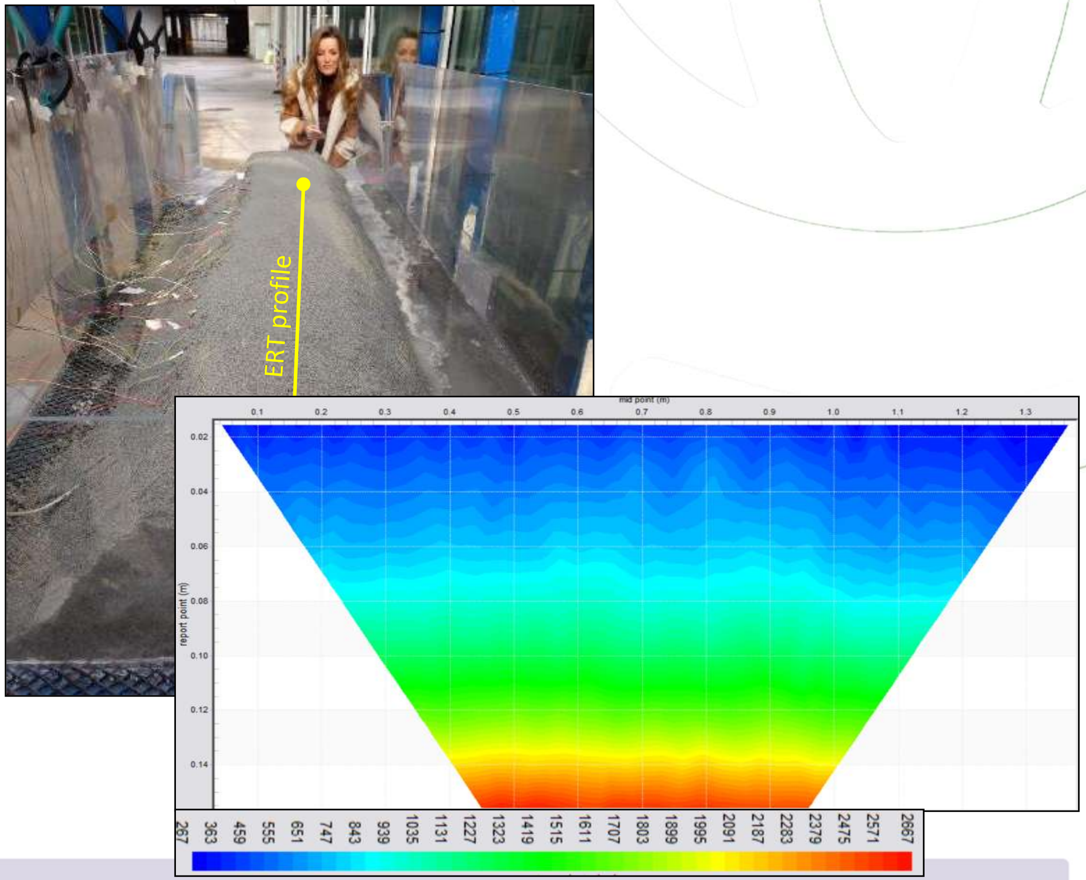

(Hojat et al., 2020; Hojat 2024)

Interpretation challenges: 3D effects

Proposed method to correct 3D effects

Data

Measured apparent resistivity pseudosection (includes 3D effects)

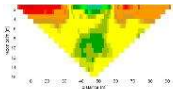

2D model of embankment (at each time)

Calculated apparent resistivity pseudosection (not accounts for 3D effects)

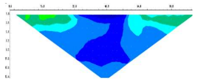

3D model of embankment and its boundary conditions (at each time)

Calculated apparent resistivity pseudosection (includes 3D effects)

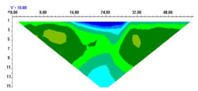

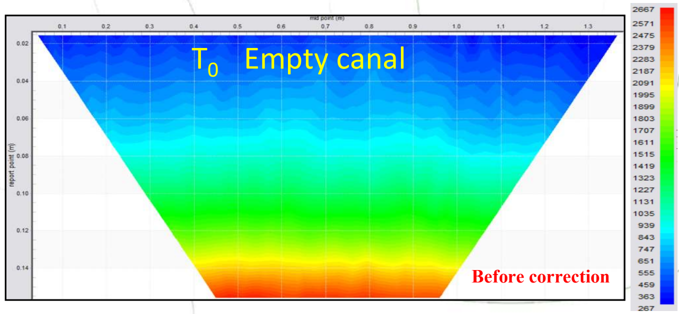

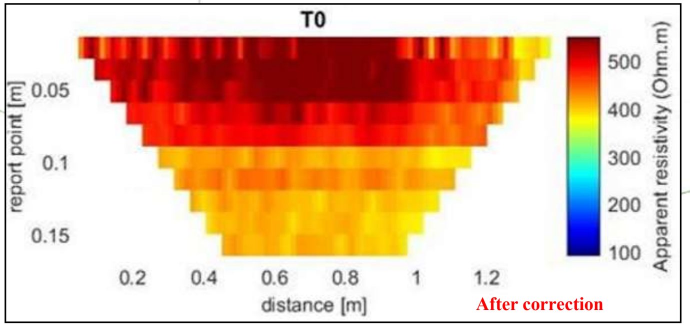

3D effects =

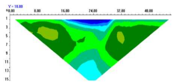

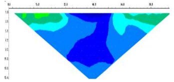

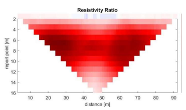

Corrected data =

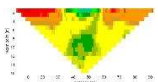

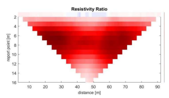

=

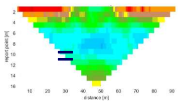

(Hojat et al., 2020)

Interpretation challenges: Time-lapse inversion

Inversion artifacts can appear when analysis the monitoring data after rainfall or drying events, i.e., the resistivity values are decreased only in some parts along the ERT line, but they are increased in other parts after rainfalls. Opposite behavior occur during the drying processes following the rainfall events.

Individual inversions

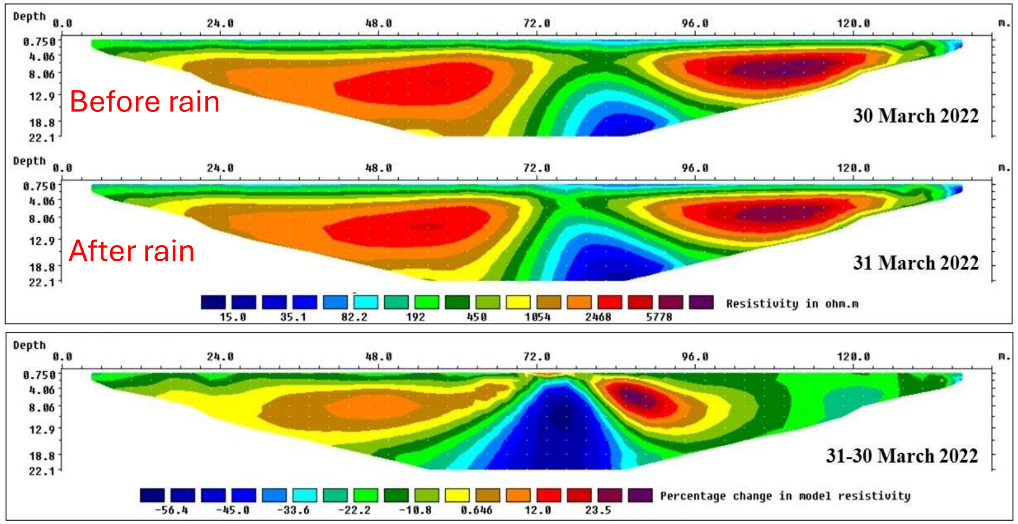

Time-lapse inversions

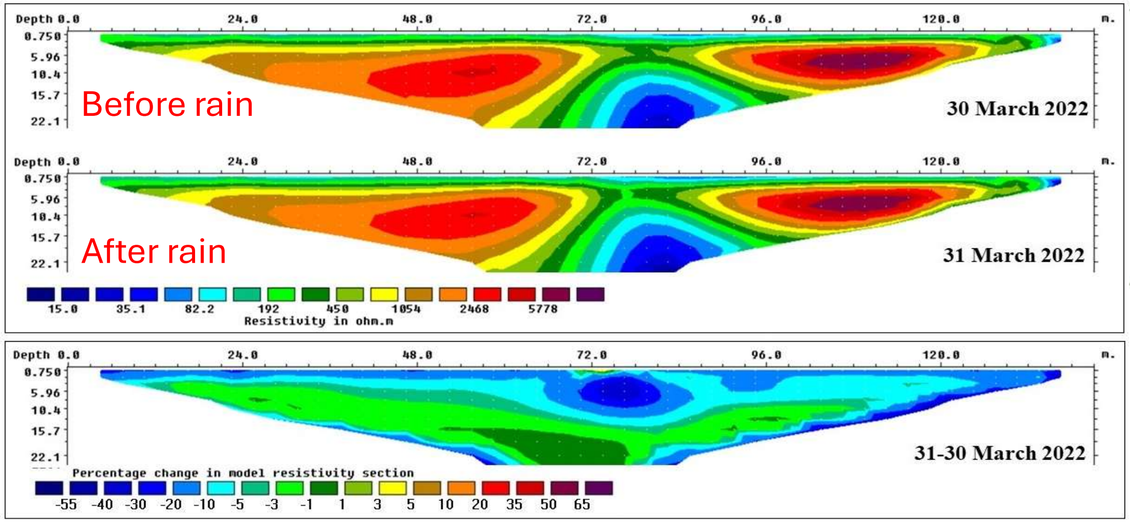

(Hojat et al., 2024)

Interpretation challenges: Temperature variations

Temperature has a minor but not negligible influence on resistivity variations, especially at shallow depths.

A model of soil temperature versus depth is used to correct resistivity sections for temperature variations in the different seasons.

$$T(z,t) = T_{mean}(air) + Ae^{-(z/d)} \sin(\omega t + \Phi - kz/d)$$

T(z,t): modelled soil temperature at depth z and on day t of the year (from 1 to 365)
$T_{mean(air)}$: mean air temperature along the entire year
A: maximum variation from the mean temperature
d: characteristic depth of penetration of temperature variations
ω: angular frequency (2π/365)
ϕ: phase
K: constant

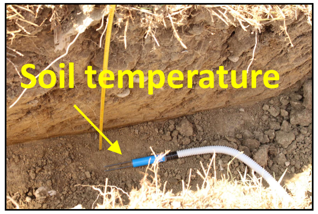

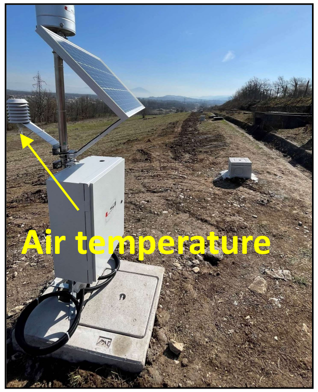

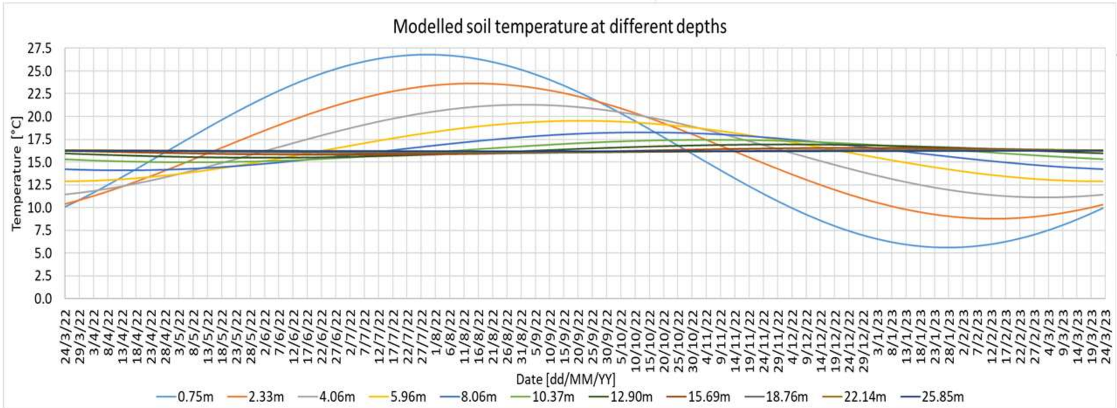

(Tresoldi et al., 2019)

Interpretation challenges: property transformation

Homogeneous material
No clays

Calibrating Archie's coefficients
Water saturation at one point is required (e.g., from TDR)

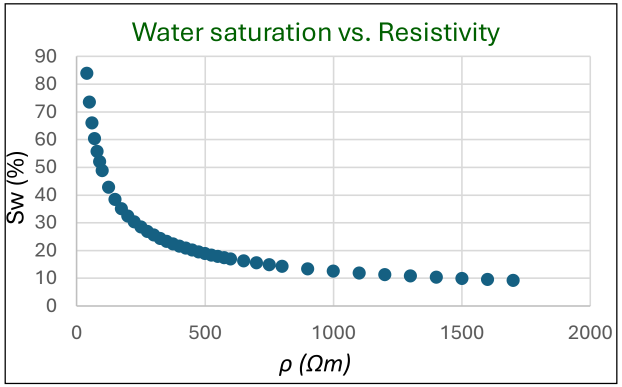

(Hojat et al., 2019)

Non-complex sites
Samples available

Fitting a power curve

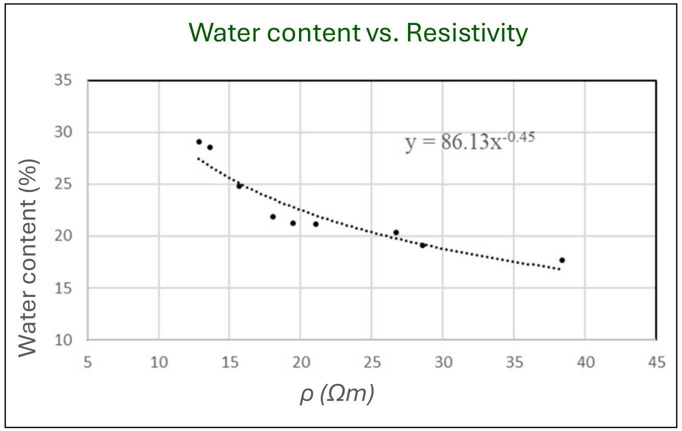

(Tresoldi et al., 2019)

Complex sites
Limited samples

Calibrating the Waxman and Smits equation (1968)

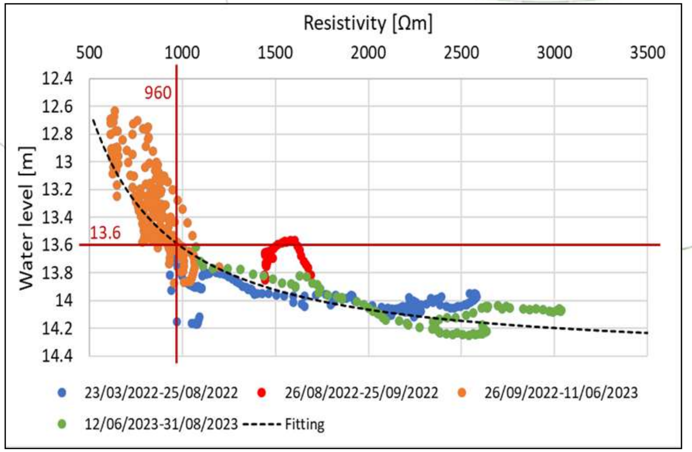

(Bianchi et al., 2024)

ITINERIS

Geophysical methods in geoscience and near surface geophysics - Electrical Prospecting

Pisa, 21 January 2025

THANKS!

Azadeh Hojat (azadeh.hojat@polimi.it)

IR0000032 – ITINERIS, Italian Integrated Environmental Research Infrastructures System
(D.D. n. 130/2022 - CUP B53C22002150006) Funded by EU - Next Generation EU PNRR-Mission 4 "Education and Research" - Component 2: "From research to business" - Investment 3.1: "Fund for the realisation of an integrated system of research and innovation infrastructures"

Finanziato dall'Unione europea NextGenerationEU
Ministero dell'Università e della Ricerca
Italiadomani